Science Advances
AAAS

Supplementary Materials for

Self-adaptive photochromism

Fanxi Sun *et al.*

Corresponding author: Yonghao Zheng, zhengyonghao@uestc.edu.cn; Chen Wei, cwei@uestc.edu.cn; Dongsheng Wang, wangds@uestc.edu.cn

Sci. Adv. **10**, eads2217 (2024)
DOI: 10.1126/sciadv.ads2217

The PDF file includes:

Other Supplementary Material for this manuscript includes the following:

1. Synthesis

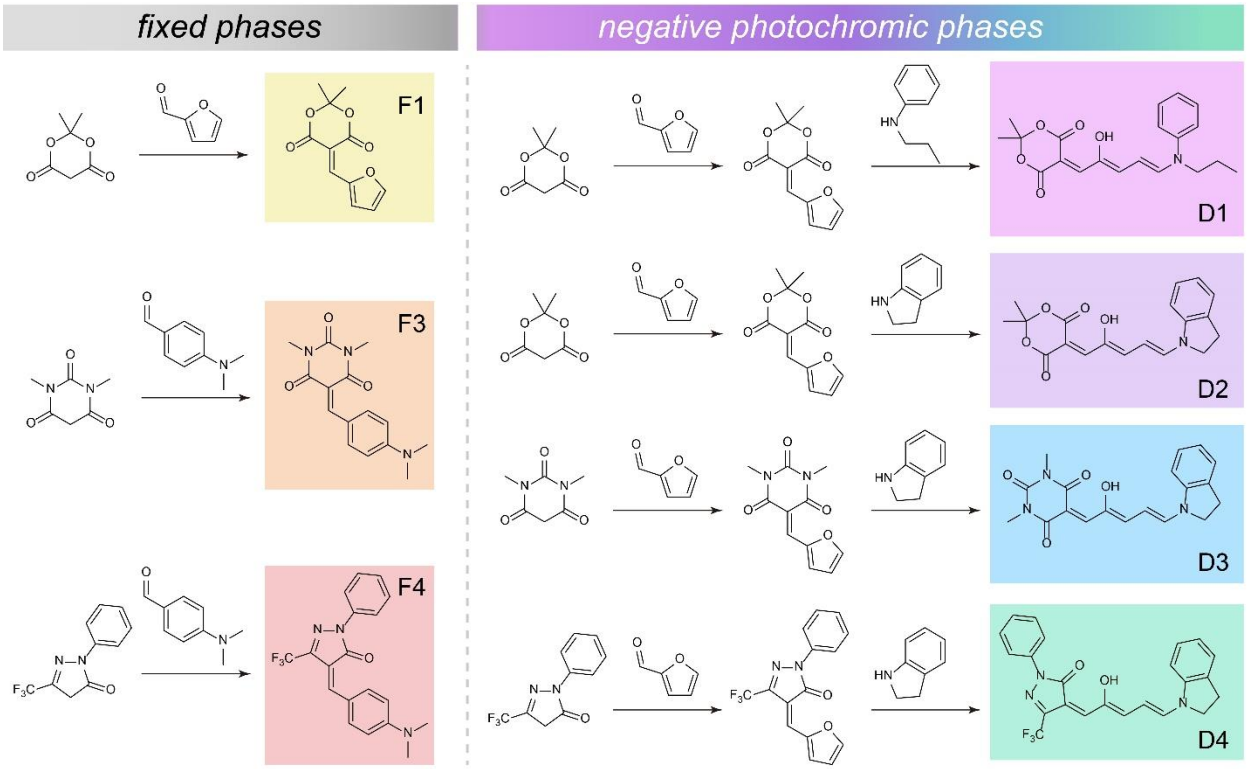

Fig. S1. Synthetic route for fixed and negative photochromic phases. Synthetic route for F1, F3, and F4 as fixed phases, and D1, D2, D3, and D4 as negative photochromic phases.

The synthesis of the color-contributing units was shown in **Fig. S1**.

Synthesis of F1. 2,2-dimethyl-1,3-dioxane-4,6-dione (1.44 g, 10 mmol) was dissolved into 30 mL distilled water under stirring. After slowly dropping 2-furaldehyde (0.96 g, 10 mmol), the solution was heated to 40^{o}C and kept for 2 h. The formed yellow solid was collected by vacuum filtration, followed by washing with distilled water. The solid was dissolved into 30 mL DCM and sequentially washed with 30 mL saturated $NaHSO_3$ aqueous solution and 30 mL saturated NaCl aqueous solution for 2 times. The organic layer was dried with Na_2SO_4 and purified by column chromatography, obtaining 2.11 g yellow product (Yield: 95%). The single crystal structure of F1 is shown in **Fig. S9**.

Synthesis of F3. 1,3-dimethylbarbituric acid (1.56 g, 10 mmol) and 4-(dimethylamino)benzaldehyde (1.49 g, 10 mmol) were dissolved into 25 mL ethanol. The solution was then heated to 90 ^{o}C under vigorous sitting for 4 h. The red precipitates were collected by filtration and dried overnight to obtain 2.59 g red solid (Yield: 90%). The single crystal structure of F3 is shown in **Fig. S10**.

Synthesis of F4. 1-phenyl-3-(trifluoromethyl)-1H-pyrazol-5(4H)-one (2.28 g, 10 mmol) and 4-(dimethylamino)benzaldehyde (1.49 g, 10 mmol) were dissolved into 25 mL ethanol. The solution was then heated to 90 ^{o}C under vigorous sitting for 4 h. The red precipitates were collected by

filtration and dried overnight to obtain 3.23 g brown solid (Yield: 90%). The single crystal structure of F4 is shown in **Fig. S11**.

Synthesis of D1. F1 (1.11 g, 5 mmol) was dissolved into 50 mL DCM, followed by slowly adding n-propylaniline (0.68 g, 5 mmol). The reaction was kept stirring at 40 ^{o}C and monitored by thin layer chromatography (TLC). The mixture was condensed by rotary evaporation and further purified by column chromatography to give 0.89 g D1 as deep purple solid (Yield: 50%). The single crystal structure of D1 is shown in **Fig. S12**.

Synthesis of D2. F1 (1.11 g, 5 mmol) was dissolved into 50 mL DCM, followed by slowly adding indoline (0.60 g, 5 mmol). After stirring at 40 ^{o}C for 2 h, the solution was condensed by rotary evaporation and redissolved in the minimum amount of DCM in a 250 mL beaker. 100 mL cold hexane (-20 ^{o}C) was slowly poured into the beaker, which was then transferred to a refrigerator at -20 ^{o}C for 30 min and slowly stirred for 5 min. The purple solid was filtered and further purified by column chromatography to give 1.02 g D2 (Yield: 60%). The single crystal structure of D2 is shown in **Fig. S13**.

Synthesis of D3. 1,3-dimethylbarbituric acid (1.56 g, 10 mmol) was dissolved into 30 mL distilled water under stirring. After slowly dropping 2-furaldehyde (0.96 g, 10 mmol), the solution was heated to 40 ^{o}C and kept for 2 h. The formed yellow solid was collected by vacuum filtration, followed by washing with distilled water. The solid was dissolved into 30 mL DCM and sequentially washed with 30 mL saturated $NaHSO_3$ aqueous solution and 30 mL saturated NaCl aqueous solution for 2 times. The organic layer was dried with Na_2SO_4 and purified by column chromatography, obtaining 1.99 g yellow product as the intermediate (Yield: 85%).

The intermediate (1.17 g, 5 mmol) was dissolved into 50 mL DCM, followed by slowly adding indoline (0.60 g, 5 mmol). After stirring at 40 ^{o}C for 2 h, the solution was condensed by rotary evaporation and redissolved in the minimum amount of DCM in a 250 mL beaker. 100 mL cold hexane (-20 ^{o}C) was slowly poured into the beaker, which was then transferred to a refrigerator at -20 ^{o}C for 30 min and slowly stirred for 5 min. The dark blue solid was filtered and further purified by column chromatography to give 0.88 g D3 (Yield: 50%). The single crystal structure of D3 is shown in **Fig. S14**.

Synthesis of D4. 1-phenyl-3-(trifluoromethyl)-1H-pyrazol-5(4H)-one (2.28 g, 10 mmol) and 2-furaldehyde (0.96 g, 10 mmol) were dissolved into 30 mL DCM and stirred for 2 h at 40 ^{o}C. The mixture was condensed by rotary evaporation, which was washed with water and further purified by column chromatography to give 2.45 g intermediate as dark red solid (Yield: 80%).

The intermediate (1.53 g, 5 mmol) was dissolved into methanol at 20 ^{o}C, followed by slowly adding Indoline (0.60 g, 5 mmol). Green crystal-like solid slowly precipitated from the dark blue solution, which was filtered and washed serval times with cold methanol. The solid was collected and dried overnight to give 1.47 g D4 (Yield: 70%). The single crystal structure of D4 is shown in **Fig. S15**.

2. Photoisomerization of DASAs

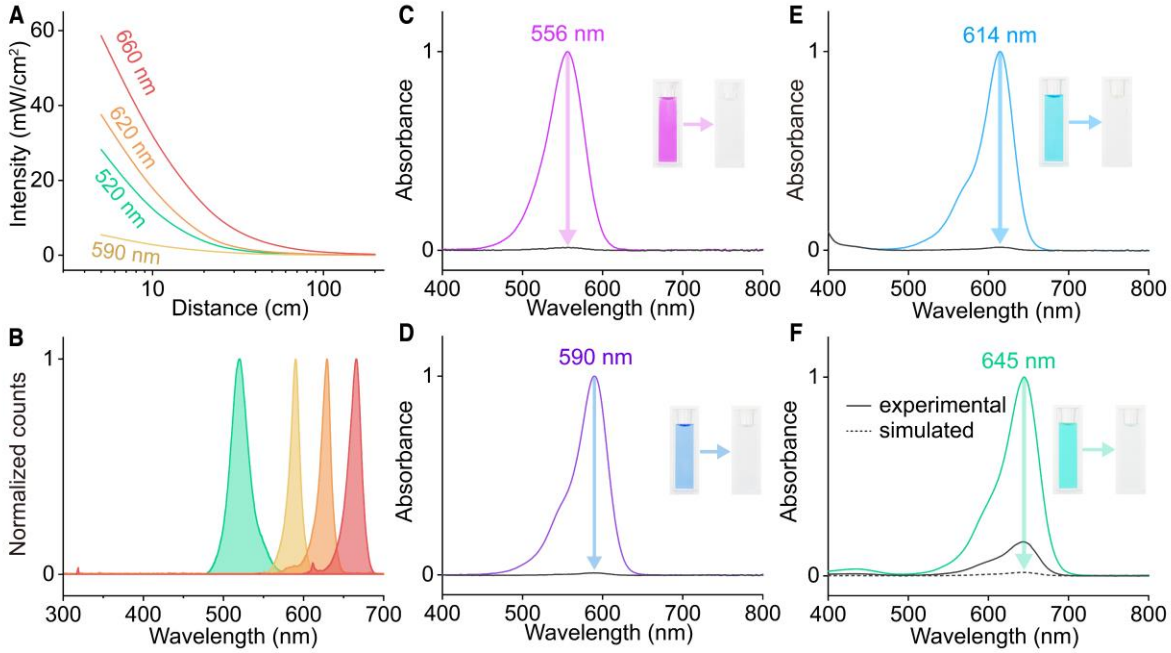

Fig. S2. Light source information and the absorption spectra of DASAs. (**A**) Relationships between light intensity and distance. (**B**) Normalized luminescence spectra of LED light sources of 520 nm, 590 nm, 620 nm, and 660 nm. (**C**-**F**) UV-vis absorption spectra of D1, D2, D3, and D4 before and after visible light irradiation (inner shows the photographic images of the photochromism).

Table S1. Information of the light sources. Relationships between light intensity and distance.

Distance/ cm	Intensity/ mW • cm^{-2}			
	520 nm	590 nm	620 nm	660 nm
5	28.21	5.49	37.53	58.60
10	10.79	2.60	16.34	30.16
20	3.18	1.15	4.67	12.44
30	1.51	0.62	2.15	6.74
40	0.86	0.38	1.28	4.22
50	0.54	0.26	0.86	2.90
60	0.39	0.19	0.63	2.13
70	0.28	0.14	0.49	1.59
75	0.26	0.13	0.41	1.42
80	0.22	0.11	0.36	1.26
90	0.18	0.09	0.28	1.03
100	0.14	0.08	0.23	0.85
130	0.09	0.05	0.14	0.53
150	0.07	0.04	0.10	0.41
200	0.04	0.02	0.06	0.26

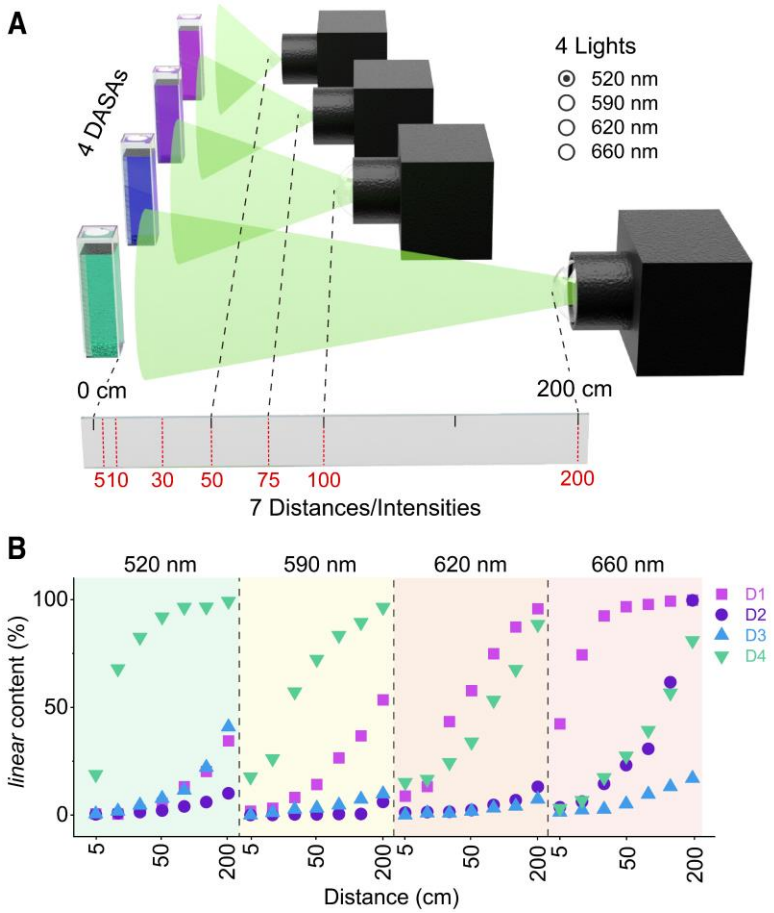

Fig. S3. Experimental setup and results for testing the linear content of DASAs under different light conditions. (**A**) Schematic illustration of the experimental setup for testing the dynamics of isomerization of DASAs under light irradiation with different wavelengths and intensities. The intensity was varied by controlling the distance between the samples and LEDs. (**B**) *linear* content (%) of DASAs at equilibrium under 520 nm, 590 nm, 620 nm, and 660 nm light irradiation. The distance between the sample and the LEDs was kept between 5 cm and 200 cm.

Preparation of DASAs solutions. PCL was dissolved into the mixed solvent of DCM and THF (9:1, v/v) with the concentration of 0.1 g/mL under stirring. DASAs were dissolved into the mixture with a specific concentration to make the initial absorbance between 0.5 and 1.5, ensuring the accuracy of the spectrophotometer, which was sealed and stored at room temperature in the dark.

Experimental setup. LED lights with the emission wavelength at 520 nm (green), 590 nm (yellow), 620 nm (orange), and 660 nm (red) were used to induce the *linear*-to-*cyclic* isomerization of DASAs (D1-D4). The interrelationship between the intensity of irradiation and distance was monitored with an illuminometer (**Fig. S2**). The distance between the sample and LEDs were set

as 5 cm, 10 cm, 30 cm, 50 cm, 75 cm, 100 cm, and 200 cm (**Fig. S3**). The temperature was maintained at 25 °C. Each kinetic measurement lasts 1800 s.

Data processing. DASAs in *cyclic* do not absorb in the visible light region, therefore, the *linear*-to-*cyclic* isomerization induces the decrease in absorbance. Based on the Lambert-Beer law, the absorbance is linearly dependent with the concentration. Therefore, the portion of *linear* DASAs at any given time (L_t) was obtained by the following equation.

$$L_t = \frac{A_t - A_{baseline}}{A_{0\,s} - A_{baseline}} \times 100\% \quad (3)$$

The *linear* DASAs content (%) at equilibrium(L_e) is obtained by fitting (equation 1) except in three scenarios 1) when the R-square is lower than 90%; 2) when the fitted *linear*% is negative (slightly lower than zero); 3) when the first-order exponential function is not applicable to describe *linear*-to-*cyclic* isomerization, for example, while using an irrelevant light to irradiate the DASAs that has no or little absorption in corresponding wavelength at low intensity (irradiating D1 with 660 nm at 200 cm), no or little isomerization occurs. For these invalid fitting data, the *linear*% at equilibrium($L_{e'}$) is obtained by only considering the starting($L_{0\,s}$) and ending($L_{1800\,s}$) *linear%*, by following equation.

$$L_{e'} = \frac{L_{1800\,s}}{L_{0\,s}} \times 100\% \quad (4)$$

The raw data of absorbance and transformed *linear* content at each time interval are shown in **Table S4-S32**.

3. Optimizing the SAP materials

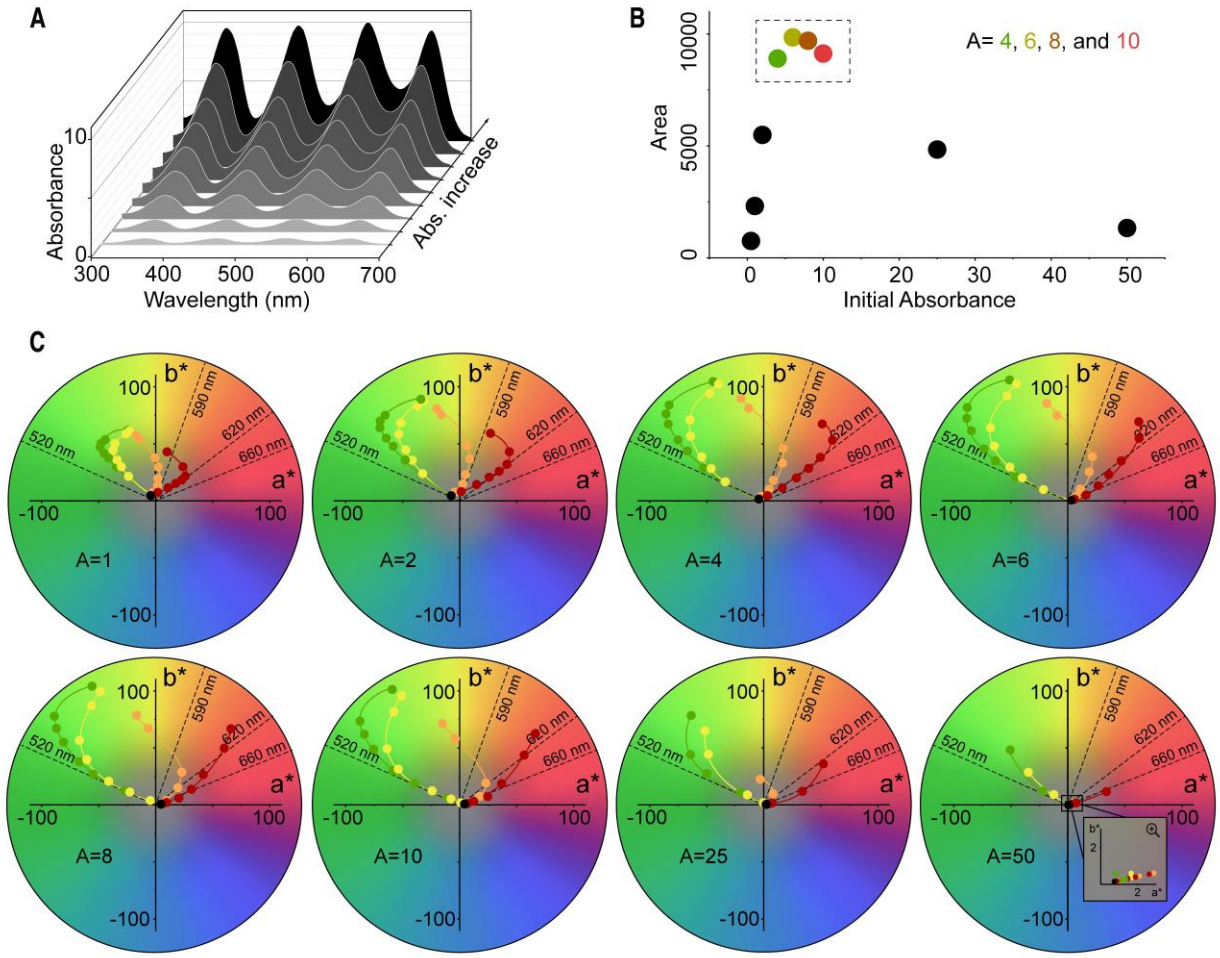

Fig. S4. Color tunability of A4 solutions under varied light conditions. (**A**) Simulated UV-vis absorption spectra of A4 solutions with the initial absorbance increasing from 0.5 to 10 (A=25 and 50 are not shown). (**B**) Summarized tunable range of color for A4 solutions. (**C**) Modified CIE 1931 *a*b** values of A4 solutions (Abs=0.5, 1, 2, 4, 8, 10, 25, and 50) under 520 nm (green), 590 nm (yellow), 620 nm (orange), and 660 nm (red) light irradiation, the distance was kept at 5 cm, 10 cm, 30 cm, 50 cm, 75 cm, 100 cm, 200 cm, dash lines stand for the color of LED lights.

Obtain the L, a*, b* values.* The simulated transmission spectra of SAP solutions were input into the plugin of OriginLab (Chromaticity Diagram, Transmittance (0-1), mode D65, Standard Observer CIE 1931 2°) to obtain the *L**, *a**, *b** values. To make a direct investigation on the color, the *a* b** coordinates were constructed in the chromaticity diagram. For the selection of color-contributing units, the *L**, *a**, *b** values of the SAP solutions of A2, A4, A6, R6, A8, and R8 were calculated (**Table S34**). Besides, A4 solutions with the initial absorbance between 0.5 and 50 were investigated (**Table S35**). For the investigation of the SAP solutions under light irradiation, the cumulative absorption spectra were calculated via the equilibrated *linear* content (%) of D1 and D4, the data were obtained from **Fig. 1E**, **Fig. S3B** and **Table S32**. The absorption and transmission spectra of the SAP solutions were recorded in **Fig. S19-S27**, which were further transferred into the *L**, *a**, *b** values and recorded in the chromaticity diagram (**Table S36-S44** and **Fig. 3A** and **Fig. S4C**).

Determine the accuracy of color. The accuracy of color without light irradiation (black state) was determined by the sum of *L** and SQRT(a^{*2}+b^{*2}), which represent lightness and deviation, respectively. The SQRT(a^{*2}+b^{*2}) was obtained through the following equation.

$$SQRT(a^{*2} + b^{*2}) = \sqrt{a^{*2} + b^{*2}} \quad (5)$$

The absorption spectra of A4 under light irradiation with different wavelengths and intensities were calculated by accumulating the spectra of color-contributed units at photostationary state through the following equation.

$$A = a\varepsilon_{F1} + c\varepsilon_{F3} + e[L_{eD1}\varepsilon_{lD1} + (1 - L_{eD1})\varepsilon_{cD1}] + h[L_{eD4}\varepsilon_{lD4} + (1 - L_{eD4})\varepsilon_{cD4}] \quad (6)$$

L_{eD1} and L_{eD4} represent the *linear* content at equilibrium for D1 and D4; ε_{lD1}, ε_{cD1}, ε_{lD4} and ε_{cD4} represent the molar absorption coefficients for *linear* D1, *cyclic* D1, *linear* D4 and *cyclic* D4, respectively. Theoretically, the ε_{cD1} and ε_{cD4} are equal to 0 between the wavelengths of 400 and 700 nm, due to the dispersed conjugation of *cyclic* DASAs. The information of calculated absorbance spectra was shown in **Fig. S19-S27**.

In the chromaticity diagram, the color of SAP solutions after light irradiation is recorded with a dot with specific *a*b** values, while the color of light is recorded with a straight line across the origin of coordinate. The direction of the line is determined according to the emission spectra of the LEDs(**Fig. S2B**). The accuracy of color under light irradiation (colored state) was determined by the difference of angle (Δθ) in the chromaticity diagram between the SAP solutions (dot, θ_D) and corresponding light (line, θ_L). For any dot with a specific *a*b** value, the θ_D could be calculated by the following equation.

$$\theta(a^*, b^*) = \begin{cases} arctan(b^*/a^*), & b^*/a^* > 0 \\ arctan(b^*/a^*) + 180, & b^*/a^* < 0 \end{cases} \quad (7)$$

Sequentially, the Δθ could be obtained by the following equation, and the results were recorded in **Table S47-S55**.

$$\Delta\theta = \theta_D - \theta_L \quad (8)$$

4. Active camouflage of SAP solutions

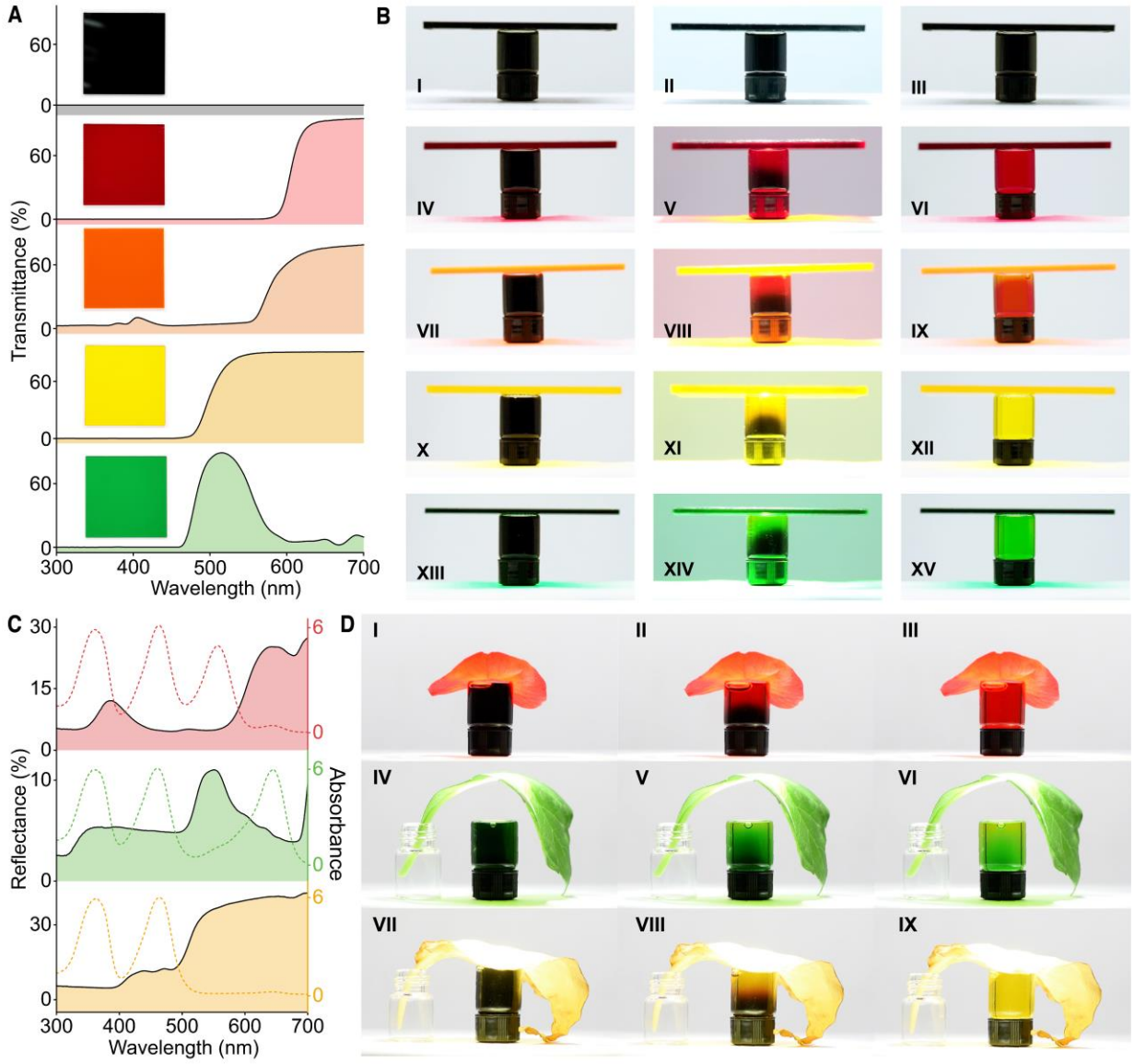

Fig. S5. Color-changing behavior of SAP solutions under various acrylic plates and natural materials. (**A**) Transmission spectra and images of red, orange, yellow and green acrylic plates. (**B**) Video screenshots of the self-adaptive color-changing process of SAP solutions under red, orange, yellow and green acrylic plates. (**C**) UV-vis diffuse reflectance spectra of *Cyclamen persicum* (red), *Epipremnum aureum* (green), and *Ginkgo* (yellow) and the UV-vis absorption spectra of the corresponding SAP solutions. (**D**) Video screenshots of the self-adaptive color-changing process of SAP solutions under red petal, green leaf and yellow leaf.

Preparation of SAP solutions. The color-contributing units were dissolved into the mixture of PCL, DCM and THF to prepare SAP solutions. A4 with the initial absorbance of 6 was selected for the

fabrication. F1, F3, D1 and D4 were dissolved into the mixed solvent, while the absorbance at 362 , 461 , 556 and 645 nm were kept at 3 (in a 0.5 cm cuvette). Due to the spontaneously occurred *linear*-to-*cyclic* isomerization of D1, the absorbance at 556 nm decreases sharply at the end of the first day (**Fig. S28A-B**). The absorbance at 556 nm keeps decreasing the in the second and third day, which however is less than the first day. Therefore, we used a "little and often" strategy to prepare the SAP solutions. After the first day, a small amount of D1 was added to make the absorbance at 556 nm reaches 3 again (**Fig. S28C-D**). This step was repeated at the third day. The absorbance does not obviously change after 3 days (**Fig. S28E-F**). The SAP solutions were sealed and stored in the dark under room temperature.

Processing of the video for active camouflage. The video of active camouflage with acrylic boxes was processed to quantitatively determine the camouflage property of SAP solutions. The LAB color space is based on the human eye's perception of colors and represent all the colors those the human eyes can perceive. "L" represents the lightness, "A" represents the red-green color difference, and "B" represents the blue-yellow color difference. The total color difference (ΔE) between the two colors is calculated as the following equation.

$$\Delta E = \sqrt{\Delta L^2 + \Delta A^2 + \Delta B^2} \tag{9}$$

To make the calculation simpler, we used a weighted Euclidean distance formula in RGB color space to determine the color difference, as shown in equations S7-S9.

$$\overline{r} = \frac{C_{1,R} + C_{2,R}}{2} \tag{10}$$

$$\begin{cases} \Delta R = C_{1,R} - C_{2,R} \\ \Delta G = C_{1,G} - C_{2,G} \\ \Delta B = C_{1,B} - C_{2,B} \end{cases} \tag{11}$$

$$\Delta C = \sqrt{\left(2 + \frac{\overline{r}}{256}\right) \times \Delta R^2 + 4 \times \Delta G^2 + \left(2 + \frac{255 - \overline{r}}{256}\right) \times \Delta B^2} \tag{12}$$

In this formula, $\overline{r}$ is the average value of the red channel of colors $C_{1,R}$ and $C_{2,R}$ (C_1 and C_2 represent any two channels in the video for comparison), ΔR is the difference between the red channel values of colors $C_{1,R}$ and $C_{2,R}$, ΔG is the difference between the red channel values of colors $C_{1,R}$ and $C_{2,R}$, ΔB is the difference between the red channel values of colors $C_{1,R}$ and $C_{2,R}$.

To eliminate the side effects in the video such as reflection on the cuvette, rectangular regions with the size of 10*40 pixels were selected on both the samples (SAP solution and black ink) and on the acrylic box (as the background), respectively (**Fig. 4D**). For each frame of the video, the average values of the R, G, and B channels within the selected rectangular region were calculated. The color difference on the SAP solution (A), background (B), and black ink (C) were calculated. The source code for the processing of video is available.

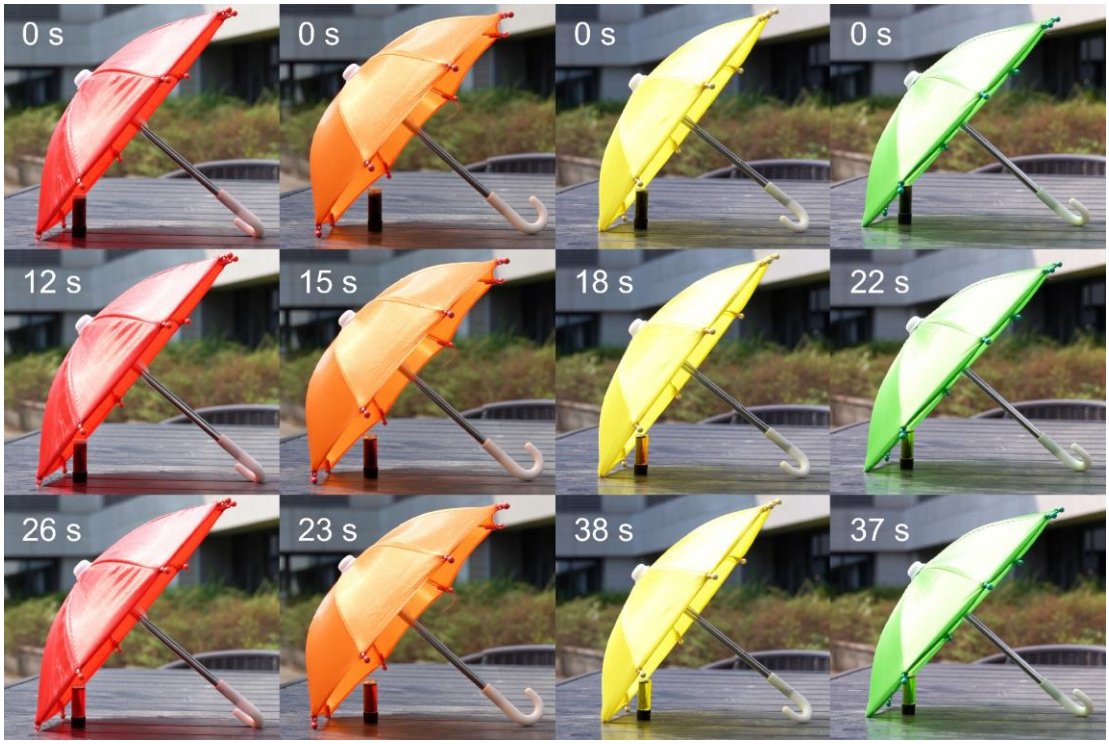

Fig. S6. Color-changing behavior of SAP solutions under transmitted sunlight. Photographic images of hiding SAP solutions into red, orange, yellow and green umbrellas under sunlight.

5. SAP in the solid state

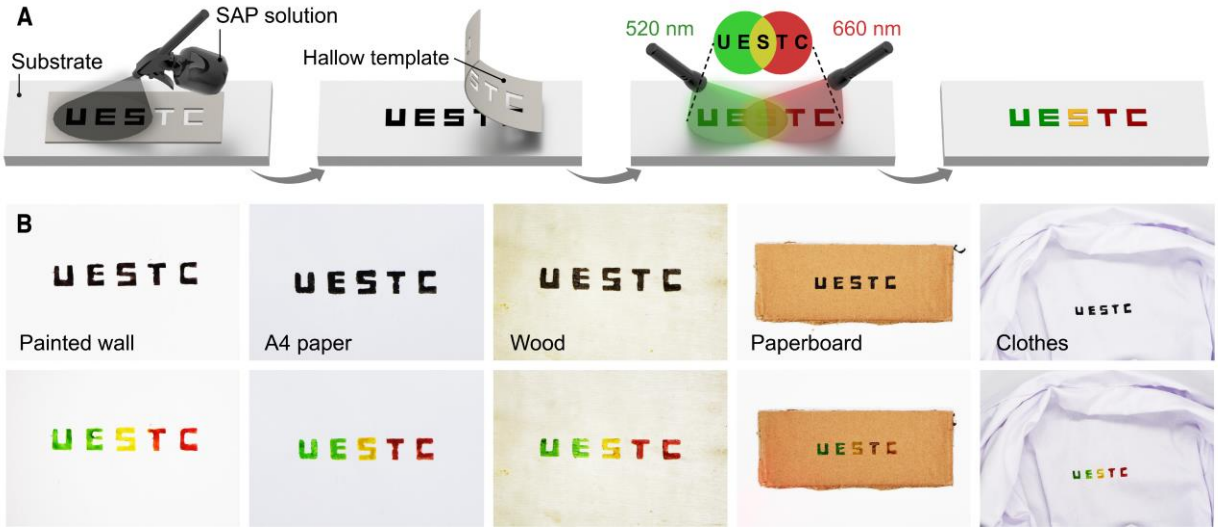

Fig. S7. Color-changing behavior of SAP coatings on different surfaces. (**A**) Schematic illustration of the mask-assisted spray-coating process and irradiation method of green light (520 nm), red light (660 nm) and mixed yellow light. (**B**) Images of SAP coating on rough surfaces (painted wall, A4 paper, wood, paperboard and clothes), images of the above surfaces irradiated by green light(520 nm), red light(660 nm) and mixed yellow light.

Fabrication of SAP films. The SAP film was fabricated by spin-coating with the rotate speed of 500 rpm, rotational acceleration of 100 rpm/s and spin coating time of 60 s. Glass was used as the substrate. After spin-coating, the substrate was annealed in the vaccum oven at 80 ^{o}C for 30 min, obtaining a relatively flat and smooth surface. The film was carefully peeled off from the glass substrate.

Coating on figurine models. The SAP coatings were prepared in a similar procedure with that for the SAP solutions. The SAP coatings were spray-coated onto the surface of figurine models made of ABS. A commercial spray-coating suit was used, the nozzle diameter is 0.5 mm, the distance between the tube and model is kept at 3 cm, the air pressure is set between 15-30 psi. During the spray-coating, the moving speed of the spraying gun is controlled at 5 cm/s. The spray-coating is repeated for 10 times to make the film thick enough (**Fig. S29**). After coating, the substrates were annealed by a temperature-adjustable heat gun at 150 ^{o}C for 10 s, which generates a smooth surface (**Fig. S30**).

6. Crystal structure of color-contributing units

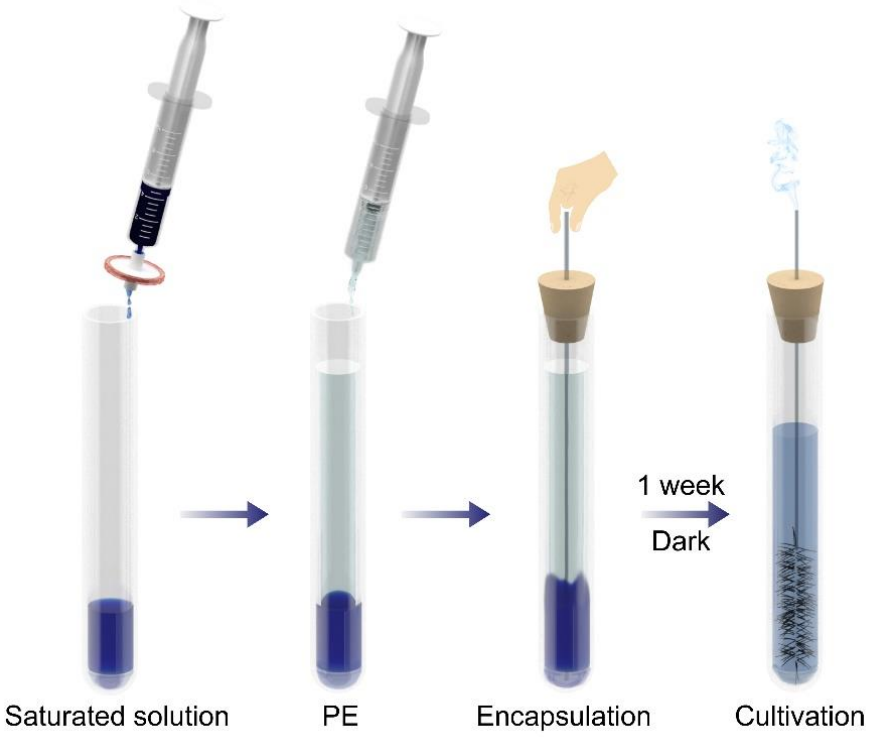

Fig. S8. Single-crystal growth of color-contributing units. Schematic illustration of single-crystal growth process.

The single-crystal growth for all the color-contributing compounds is similar (**Fig. S8**). Taking D4 as the example, 3 mL saturated solution of D4 in DCM was filtered through a Teflon filter and injected into a 20 mL glass tube. 15 mL petroleum ether (PE) was carefully added along the wall of the tube without disturbing the surface of the saturated solution. The tube was sealed with a rubber plug. A capillary tube longer than the above glass tube and with an inner diameter of 0.5 mm was slowly punctured through the plug and inserted into the bottom of the glass tube. The tube was placed in the dark for 1 week to evaporate most of the DCM. Crystals with color and fixed morphology are selected for further characterization. The crystal structure data of F1, F3, F4 and D1-D4 were shown in **Fig. S9-S15**.

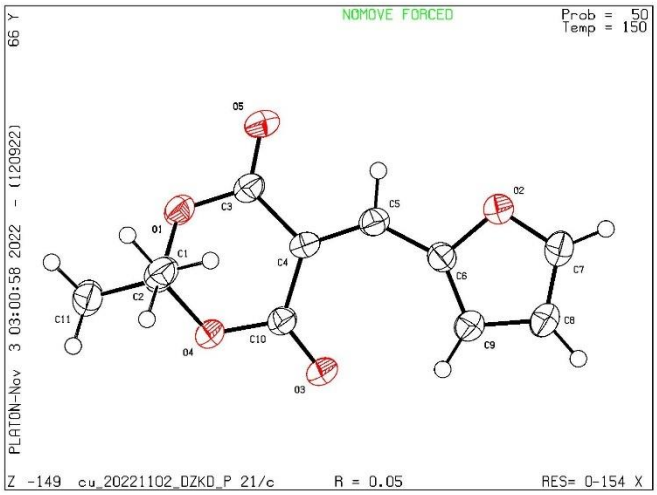

Fig. S9. Crystal structure data for 5-(furan-2-ylmethylene)-2,2-dimethyl-1,3-dioxane-4,6-dione (F1). Detailed information can be obtained free of charge from the Cambridge Crystallographic Data Centre via www.ccdc.cam.ac.uk/data_request/cif CCDC# 2258709

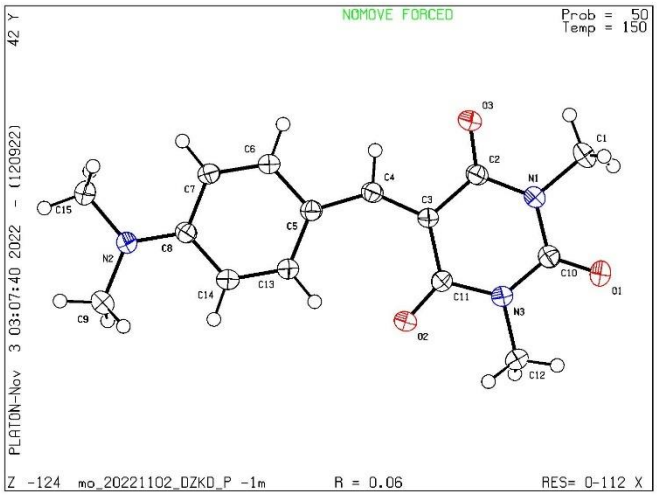

Fig. S10. Crystal structure data for 5-(4-(dimethylamino)benzylidene)-1,3-dimethylpyrimidine-2,4,6(1H,3H,5H)-trione (F3). Detailed information can be obtained free of charge from the Cambridge Crystallographic Data Centre via www.ccdc.cam.ac.uk/data_request/cif CCDC# 2258710

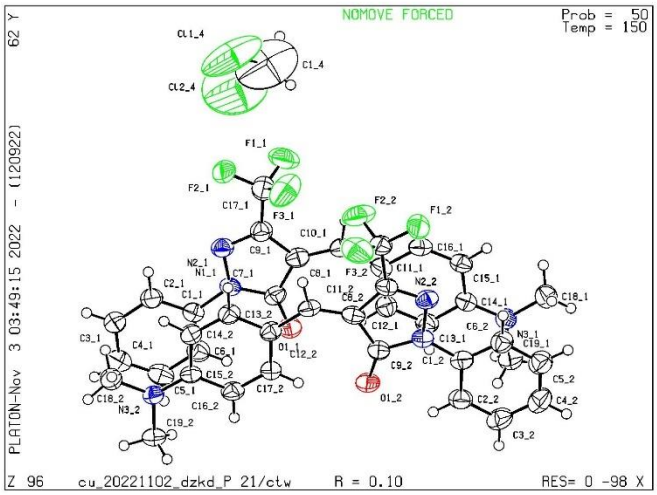

Fig. S11. Crystal structure data for (Z)-4-(furan-2-ylmethylene)-2-phenyl-5-(trifluoromethyl)-2,4-dihydro-3H-pyrazol-3-one (F4). Detailed information can be obtained free of charge from the Cambridge Crystallographic Data Centre via www.ccdc.cam.ac.uk/data_request/cif CCDC# 2258708

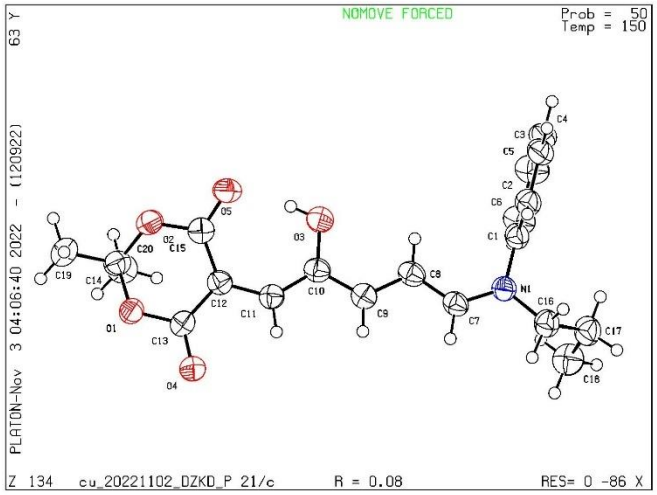

Fig. S12. Crystal structure data for 5-((2Z,4E)-2-hydroxy-5-(phenyl(propyl)amino)penta-2,4-dien-1-ylidene)-2,2-dimethyl-1,3-dioxane-4,6-dione (D1). Detailed information can be obtained free of charge from the Cambridge Crystallographic Data Centre via www.ccdc.cam.ac.uk/data_request/cif CCDC# 2258697

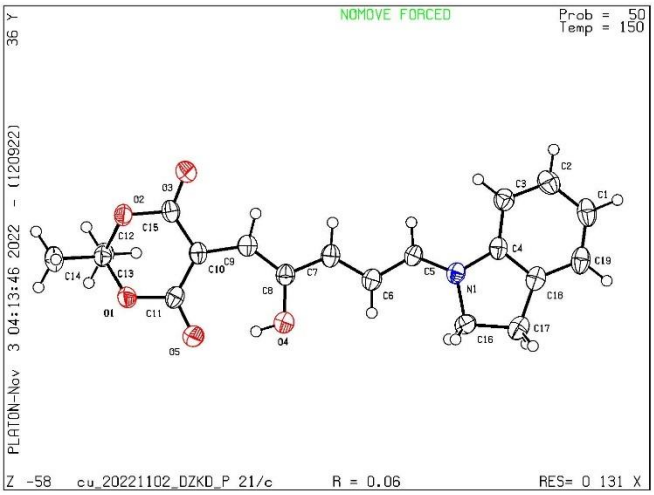

Fig. S13. Crystal structure data for 5-((2Z,4E)-2-hydroxy-5-(indolin-1-yl)penta-2,4-dien-1-ylidene)-2,2-dimethyl-1,3-dioxane-4,6-dione (D2). Detailed information can be obtained free of charge from the Cambridge Crystallographic Data Centre via www.ccdc.cam.ac.uk/data_request/cif CCDC# 2258701

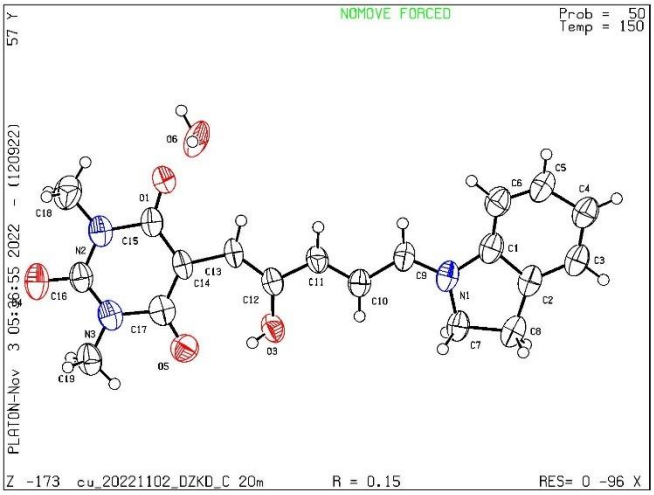

Fig. S14. Crystal structure data for 5-((2Z,4E)-2-hydroxy-5-(indolin-1-yl)penta-2,4-dien-1-ylidene)-1,3-dimethylpyrimidine-2,4,6(1H,3H,5H)-trione (D3). Detailed information can be obtained free of charge from the Cambridge Crystallographic Data Centre via www.ccdc.cam.ac.uk/data_request/cif CCDC# 2258702

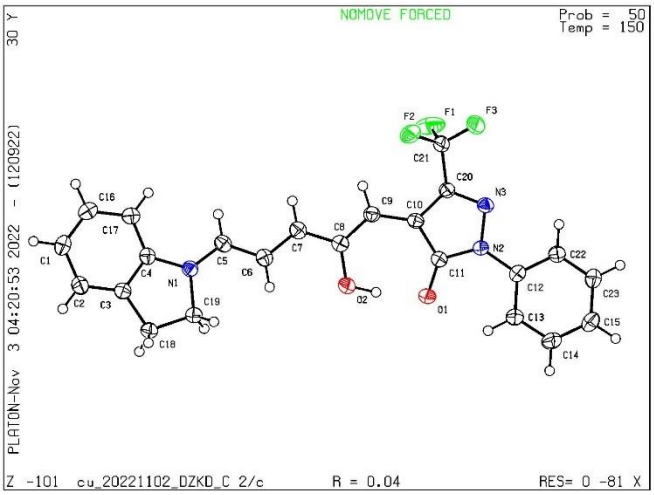

Fig. S15. Crystal structure data for (Z)-4-((2Z,4E)-2-hydroxy-5-(indolin-1-yl)penta-2,4-dien-1-ylidene)-2-phenyl-5-(trifluoromethyl)-2,4-dihydro-3H-pyrazol-3-one (D4). Detailed information can be obtained free of charge from the Cambridge Crystallographic Data Centre via www.ccdc.cam.ac.uk/data_request/cif CCDC# 2258708

7. Molar absorption coefficients for the color-contributing units

For the fixed phases F1-F4, the molar absorption coefficients were obtained right after dissolving the molecules. For photochromic phases D1-D4, the molar absorption coefficients were monitored 3 times in 3 days (**Fig. S16E-P**). The fitting results were shown in **Table S2**.

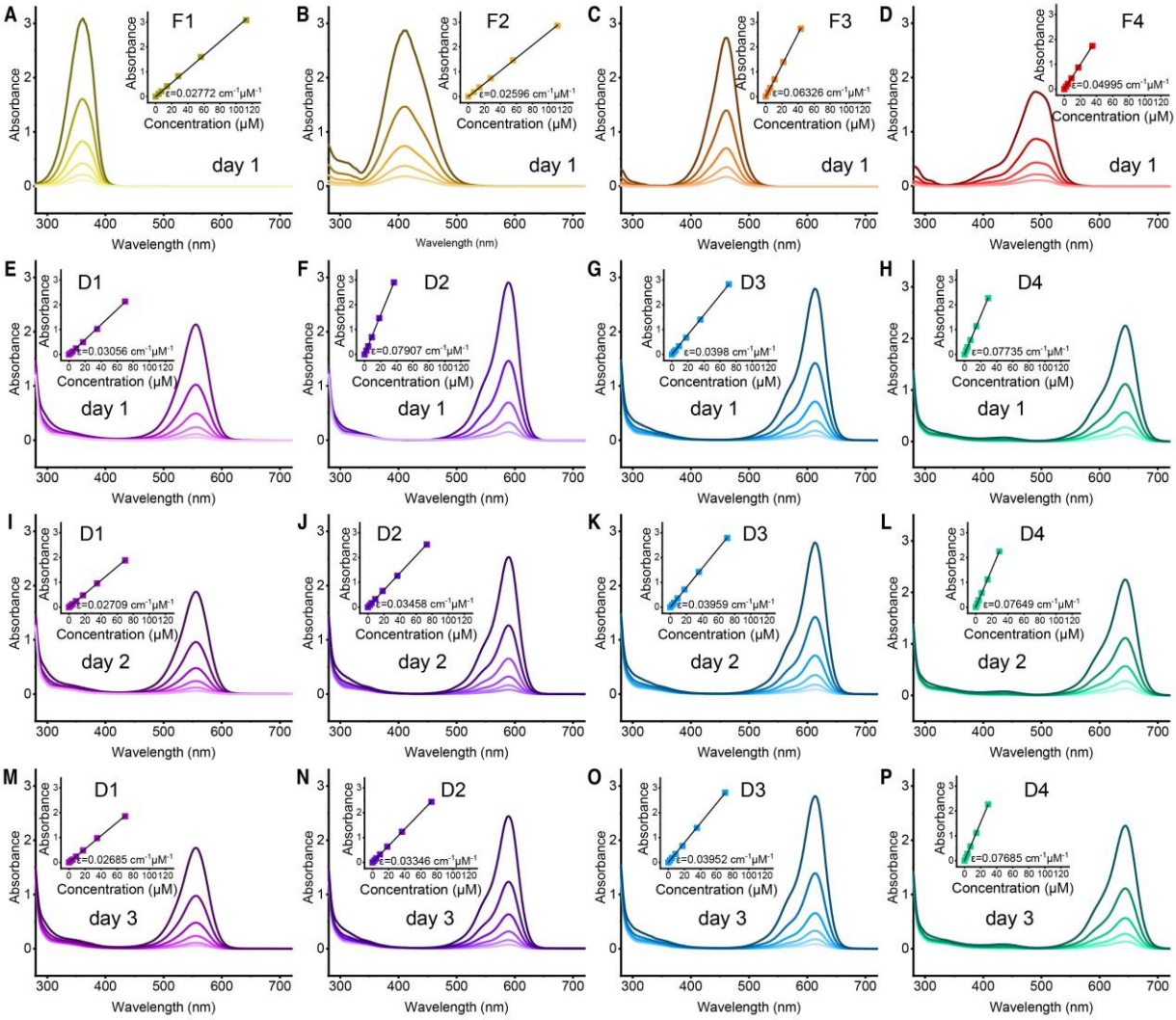

Fig. S16. UV-vis concentration vs. absorbance curves for Color-contributing units. (**A-D**) UV-vis concentration vs. absorbance curves for F1-F4. (**E-H**) UV-vis concentration vs. absorbance curves for D1-D4 on the first day. (**I-L**) UV-vis concentration vs. absorbance curves for D1-D4 on the second day. (**M-P**) UV-vis concentration vs. absorbance curves for D1-D4 on the third day.

D2 shows an obvious drop of molar absorption coefficients in the second day, which became stable in the third day. On the other hand, the molar absorption coefficients of D1, D3 and D4 are stable in 3 days (**Fig. S16-S17**). These results are attributed to the spontanouesly occurred *linear-*

to-*cyclic* isomerization. The *linear* contents (%) for D1-D4 after 3 days were summarized in **Table S3**.

Table S2. Molar absorption coefficient of the color-contributing units.

Molecule	ε/ $cm^{-1}\mu M^{-1}$	R-Square
F1	0.02772	0.9995
F2	0.02596	0.9999
F3	0.06326	0.9999
F4	0.04995	0.9999
D1-Day 1	0.03056	0.9995
D2-Day 1	0.07907	0.9997
D3-Day 1	0.0398	0.9998
D4-Day 1	0.07735	0.9999
D1-Day 2	0.02709	0.9999
D2-Day 2	0.03458	0.9999
D3-Day 2	0.03959	0.9999
D4-Day 2	0.07649	0.9999
D1-Day 3	0.02685	0.9996
D2-Day 3	0.03346	0.9999
D3-Day 3	0.03952	0.9997
D4-Day 3	0.07685	0.9999

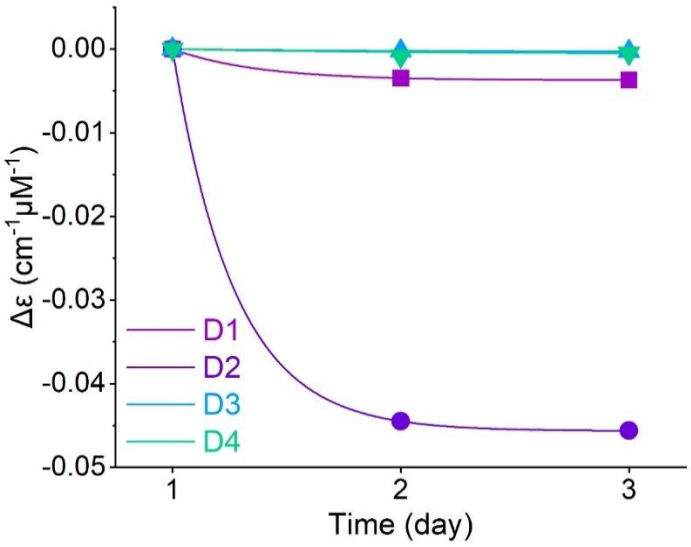

Fig. S17. Equilibrium *linear* content of D1-D4. The molar absorption coefficient loss of D1-D4 in 3 days.

Table S3. Equilibrium *linear* content of D1-D4. *linear* contents (%) of D1-D4 after keeping for 3 days.

Molecule	pristine	1st day	2nd day	3rd day
D1	100%	100	88	87
D2	100%	100	44	42
D3	100%	100	99	99
D4	100%	100	99	100

8. The *linear* content (%) of DASAs at equilibrium

Table S4. Raw data of kinetic testing. Kinetics of D1-D4 (Abs. peak) under the irradiation of 520 nm at 5 cm.

520 nm 5 cm	D1	D2	D3	D4
Abs. baseline	-0.003	-0.004	0.000	0.000
0 s	0.568	1.347	0.479	1.565
1 s	0.211	1.173	0.261	1.429
2 s	0.089	0.834	0.171	1.298
3 s	0.043	0.592	0.119	1.165
4 s	0.018	0.453	0.064	1.077
5 s	0.012	0.329	0.044	1.007
10 s	0.000	0.123	0.009	0.786
15 s	-0.001	0.055	0.004	0.640
30 s	-0.002	0.000	0.003	0.403
60 s	-0.002	-0.003	0.002	0.292
120 s	-0.002	-0.003	0.001	0.281
180 s	-0.002	-0.003	0.001	0.289
300 s	-0.002	-0.003	0.001	0.290
600 s	-0.002	-0.004	0.000	0.288
1200 s	-0.002	-0.004	0.000	0.288
1800 s	-0.002	-0.004	0.000	0.288

Table S5. Raw data of kinetic testing. Kinetics of D1-D4 (Abs. peak) under the irradiation of 520 nm at 10 cm.

520 nm 10 cm	D1	D2	D3	D4
Abs. baseline	0.002	-0.002	-0.008	0.002
0 s	0.825	1.386	0.735	0.778
1 s	0.537	0.103	0.567	0.755
2 s	0.276	0.861	0.413	0.726
3 s	0.129	0.644	0.291	0.710
4 s	0.066	0.533	0.211	0.696
5 s	0.032	0.367	0.158	0.687
10 s	0.012	0.133	0.041	0.676
15 s	0.010	0.033	0.015	0.662
30 s	0.011	0.009	0.006	0.617
60 s	0.010	0.007	0.007	0.597
120 s	0.010	0.007	0.006	0.567
180 s	0.010	0.008	0.005	0.556
300 s	0.010	0.008	0.007	0.540
600 s	0.010	0.008	0.005	--
1200 s	0.010	0.007	0.005	0.508
1800 s	0.010	0.006	0.005	0.485

Table S6. Raw data of kinetic testing. Kinetics of D1-D4 (Abs. peak) under the irradiation of 520 nm at 30 cm.

520 nm 30 cm	D1	D2	D3	D4
Abs. baseline	-0.042	-0.015	-0.004	-0.004
0 s	0.849	1.478	0.677	0.563
1 s	0.800	1.417	0.645	0.555
2 s	0.740	1.357	0.603	0.551
3 s	0.698	1.293	0.574	0.548
4 s	0.648	1.233	0.547	0.544
5 s	0.593	1.176	0.521	0.542
10 s	0.497	1.024	0.456	0.530
15 s	0.383	0.875	0.387	0.530
30 s	0.201	0.517	0.244	0.512
60 s	0.055	0.156	0.093	0.485
120 s	-0.006	0.018	0.040	0.479
180 s	--	0.010	0.029	0.474
300 s	-0.025	0.009	0.027	0.469
600 s	-0.037	0.007	0.023	0.462
1200 s	-0.036	0.008	0.024	0.466
1800 s	-0.037	0.008	0.023	0.447

Table S7. Raw data of kinetic testing. Kinetics of D1-D4 (Abs. peak) under the irradiation of 520 nm at 50 cm.

520 nm 50 cm	D1	D2	D3	D4
Abs. baseline	0.006	0.001	0.000	0.000
0 s	0.819	1.854	0.700	0.482
1 s	0.801	1.819	0.683	0.479
2 s	0.777	--	0.667	0.477
3 s	0.757	1.778	0.654	0.473
4 s	0.731	1.808	0.637	0.472
5 s	0.712	1.720	0.630	0.473
10 s	0.664	1.621	0.607	0.470
15 s	0.609	1.534	0.574	0.469
30 s	0.466	1.342	0.492	0.461
60 s	0.293	1.039	0.378	0.454
120 s	0.121	0.561	0.217	0.449
180 s	0.073	0.300	0.138	0.449
300 s	0.056	0.097	0.083	0.449
600 s	0.049	0.049	0.049	0.440
1200 s	0.051	0.045	--	0.440
1800 s	0.048	0.046	0.051	0.440

Table S8. Raw data of kinetic testing. Kinetics of D1-D4 (Abs. peak) under the irradiation of 520 nm at 75 cm.

520 nm 75 cm	D1	D2	D3	D4
Abs. baseline	0.000	0.000	0.002	0.003
0 s	1.241	1.497	0.491	0.549
1 s	--	--	0.473	--
2 s	--	--	0.466	--
3 s	--	--	0.458	--
4 s	--	--	0.452	--
5 s	1.120	1.066	0.448	0.548
10 s	1.056	0.901	0.440	0.547
15 s	0.987	0.724	0.430	0.545
30 s	0.778	0.483	0.403	0.541
60 s	0.630	0.177	0.354	0.538
120 s	0.396	0.057	0.279	0.535
180 s	0.271	0.052	0.218	0.531
300 s	0.188	0.052	0.151	0.531
600 s	0.159	0.054	0.080	0.529
1200 s	0.148	0.055	0.057	0.530
1800 s	0.148	0.053	0.055	0.529

Table S9. Raw data of kinetic testing. Kinetics of D1-D4 (Abs. peak) under the irradiation of 520 nm at 100 cm.

520 nm 100 cm	D1	D2	D3	D4
Abs. baseline	-0.004	0.000	0.009	-0.002
0 s	0.844	1.462	0.712	0.844
1 s	0.832	1.449	0.696	0.840
2 s	0.826	1.438	0.690	0.840
3 s	0.816	1.430	0.690	0.838
4 s	0.808	1.415	0.681	0.839
5 s	0.799	1.400	0.675	0.839
10 s	0.785	1.368	0.665	0.836
15 s	0.766	1.342	0.653	0.838
30 s	0.719	1.291	0.629	0.837
60 s	0.633	1.190	0.577	0.836
120 s	0.499	1.020	0.485	0.833
180 s	0.396	0.876	0.420	0.829
300 s	0.265	0.623	0.320	0.823
600 s	0.187	0.273	0.217	0.821
1200 s	0.172	0.118	0.177	0.817
1800 s	0.168	0.103	0.152	0.814

Table S10. Raw data of kinetic testing. Kinetics of D1-D4 (Abs. peak) under the irradiation of 520 nm at 200 cm.

520 nm 200 cm	D1	D2	D3	D4
Abs. baseline	0.000	0.000	-0.004	0.005
0 s	0.584	1.426	0.480	0.560
1 s	0.582	1.423	0.478	--
2 s	0.580	1.424	0.476	--
3 s	0.579	1.429	0.473	--
4 s	0.577	1.422	0.471	--
5 s	0.576	1.414	0.470	0.559
10 s	0.573	1.409	0.468	0.558
15 s	0.569	1.404	0.466	0.558
30 s	0.560	1.388	0.459	0.557
60 s	0.539	1.361	0.450	0.557
120 s	0.505	1.316	0.420	0.557
180 s	0.474	1.271	0.411	0.556
300 s	0.421	1.189	0.385	0.557
600 s	0.326	0.985	0.316	0.556
1200 s	0.258	0.706	0.251	0.555
1800 s	0.207	0.511	0.215	0.554

Table S11. Raw data of kinetic testing. Kinetics of D1-D4 (Abs. peak) under the irradiation of 590 nm at 5 cm.

590 nm 5 cm	D1	D2	D3	D4
Abs. baseline	-0.003	-0.004	0.000	0.000
0 s	0.589	1.329	0.475	1.559
1 s	0.437	1.063	0.248	1.383
2 s	0.337	0.811	0.107	1.162
3 s	0.281	0.554	0.036	0.890
4 s	0.227	0.405	0.018	0.753
5 s	0.178	0.273	0.007	0.639
10 s	0.094	0.089	0.001	0.520
15 s	0.046	0.025	0.000	0.386
30 s	0.008	-0.003	0.000	0.287
60 s	0.003	-0.004	0.000	0.278
120 s	0.003	-0.004	0.000	0.257
180 s	0.003	-0.004	0.000	0.259
300 s	0.003	-0.004	0.000	0.259
600 s	0.002	-0.004	0.000	0.257
1200 s	0.001	-0.004	0.000	0.259
1800 s	0.001	-0.004	0.000	0.259

Table S12. Raw data of kinetic testing. Kinetics of D1-D4 (Abs. peak) under the irradiation of 590 nm at 10 cm.

590 nm 10 cm	D1	D2	D3	D4
Abs. baseline	0.010	-0.002	-0.009	0.002
0 s	0.828	1.424	0.681	0.717
1 s	0.766	1.255	0.428	0.602
2 s	0.713	0.965	0.248	0.526
3 s	0.608	0.717	0.127	0.471
4 s	0.545	0.428	0.062	0.423
5 s	0.484	0.318	0.031	0.417
10 s	0.368	0.076	0.003	0.322
15 s	0.267	0.026	0.003	0.307
30 s	0.104	0.007	0.002	0.228
60 s	0.041	0.006	0.001	0.206
120 s	0.033	0.005	0.001	0.199
180 s	0.034	0.005	0.001	0.194
300 s	0.031	0.005	0.001	--
600 s	0.031	0.005	0.003	0.164
1200 s	0.031	0.006	0.001	0.150
1800 s	0.031	0.005	0.001	0.147

Table S13. Raw data of kinetic testing. Kinetics of D1-D4 (Abs. peak) under the irradiation of 590 nm at 30 cm.

590 nm 30 cm	D1	D2	D3	D4
Abs. baseline	0.001	-0.008	-0.006	-0.004
0 s	0.810	1.392	0.687	0.524
1 s	0.789	1.335	0.632	0.501
2 s	0.767	1.277	0.576	0.483
3 s	0.748	1.216	0.523	0.468
4 s	0.721	1.157	0.473	0.458
5 s	0.698	1.085	0.433	0.450
10 s	0.653	0.903	0.351	0.422
15 s	0.595	0.694	0.260	0.404
30 s	0.473	0.421	0.119	0.358
60 s	0.292	0.043	0.025	0.326
120 s	0.149	0.002	0.010	0.316
180 s	0.101	0.001	0.010	0.304
300 s	0.075	0.001	0.009	0.302
600 s	0.065	0.001	0.010	0.297
1200 s	0.055	0.000	0.008	0.284
1800 s	0.056	0.001	0.009	0.273

Table S14. Raw data of kinetic testing. Kinetics of D1-D4 (Abs. peak) under the irradiation of 590 nm at 50 cm.

590 nm 50 cm	D1	D2	D3	D4
Abs. baseline	0.006	-0.001	-0.005	0.000
0 s	0.811	1.395	0.684	0.472
1 s	0.798	1.348	0.634	0.461
2 s	0.785	1.291	0.593	0.453
3 s	0.775	1.273	0.553	0.446
4 s	0.762	1.238	0.519	0.440
5 s	0.749	1.190	0.484	0.437
10 s	0.728	1.092	0.407	0.422
15 s	0.699	0.978	0.325	0.411
30 s	0.639	0.731	0.213	0.385
60 s	0.517	0.365	0.071	0.365
120 s	0.363	0.061	0.015	0.336
180 s	0.285	0.016	0.013	0.349
300 s	0.182	0.012	0.013	0.348
600 s	0.123	0.012	0.014	0.338
1200 s	0.119	0.011	0.015	0.344
1800 s	0.113	0.011	0.013	0.328

Table S15. Raw data of kinetic testing. Kinetics of D1-D4 (Abs. peak) under the irradiation of 590 nm at 75 cm.

590 nm 75 cm	D1	D2	D3	D4
Abs. baseline	0.000	0.000	-0.003	0.003
0 s	1.245	1.490	0.466	0.547
1 s	--	--	0.448	--
2 s	--	--	0.435	--
3 s	--	--	0.415	--
4 s	--	--	0.396	--
5 s	1.183	1.271	0.381	0.531
10 s	1.166	1.167	0.351	0.519
15 s	1.146	1.045	0.315	0.506
30 s	1.106	0.782	0.248	0.492
60 s	1.019	0.392	0.147	0.475
120 s	0.866	0.068	0.059	0.458
180 s	0.758	0.020	0.029	0.455
300 s	0.591	0.016	0.019	0.454
600 s	0.416	0.016	0.015	0.448
1200 s	0.353	0.015	0.015	0.467
1800 s	0.311	0.015	0.015	0.459

Table S16. Raw data of kinetic testing. Kinetics of D1-D4 (Abs. peak) under the irradiation of 590 nm at 100 cm.

590 nm 100 cm	D1	D2	D3	D4
Abs. baseline	-0.007	0.000	-0.01	0.001
0 s	0.808	1.531	0.712	0.837
1 s	0.803	1.514	0.689	0.829
2 s	0.799	1.505	0.673	0.823
3 s	0.794	1.492	0.657	0.816
4 s	0.792	1.482	0.640	0.811
5 s	0.788	1.469	0.627	0.807
10 s	0.781	1.443	0.592	0.805
15 s	0.775	1.410	0.566	0.801
30 s	0.757	1.320	0.492	0.781
60 s	0.711	1.166	0.361	0.766
120 s	0.635	0.859	0.212	0.759
180 s	0.575	0.601	0.106	0.750
300 s	--	0.253	0.051	0.749
480 s	0.406	--	--	--
600 s	0.377	0.044	0.047	0.745
1200 s	0.322	0.034	0.047	0.745
1800 s	0.275	0.033	0.043	0.745

Table S17. Raw data of kinetic testing. Kinetics of D1-D4 (Abs. peak) under the irradiation of 590 nm at 200 cm.

590 nm 200 cm	D1	D2	D3	D4
Abs. baseline	0.000	0.000	-0.005	0.006
0 s	1.241	1.404	0.478	0.557
1 s	--	1.398	0.474	--
2 s	--	1.391	0.471	--
3 s	--	1.385	0.467	--
4 s	--	1.378	0.465	--
5 s	1.223	1.372	0.461	0.554
10 s	1.214	1.366	0.455	0.553
15 s	1.209	1.356	0.447	0.552
30 s	1.192	1.329	0.430	0.548
60 s	1.159	1.291	0.395	0.546
120 s	1.107	1.211	0.327	0.543
180 s	1.061	1.149	0.269	0.542
300 s	0.979	1.004	0.191	0.541
600 s	0.844	0.654	0.094	0.541
1200 s	0.742	0.213	0.051	0.535
1800 s	0.666	0.087	0.042	0.534

Table S18. Raw data of kinetic testing. Kinetics of D1-D4 (Abs. peak) under the irradiation of 620 nm at 5 cm.

620 nm 5 cm	D1	D2	D3	D4
Abs. baseline	0.000	-0.004	-0.003	0.000
0 s	0.563	1.349	0.468	1.557
1 s	0.553	1.233	0.163	0.971
2 s	0.465	1.112	0.037	0.474
3 s	0.452	0.974	0.008	0.331
4 s	0.444	0.861	0.001	0.302
5 s	0.434	0.756	0.000	0.282
10 s	0.411	0.561	-0.001	0.243
15 s	0.389	0.394	-0.001	0.252
30 s	0.337	0.164	-0.002	0.248
60 s	0.261	0.022	-0.002	0.241
120 s	0.162	0.000	-0.003	0.245
180 s	0.102	0.000	-0.003	0.233
300 s	0.064	0.000	-0.003	0.233
600 s	0.042	-0.001	-0.003	0.233
1200 s	0.042	-0.001	-0.003	0.233
1800 s	0.040	-0.001	-0.003	0.233

Table S19. Raw data of kinetic testing. Kinetics of D1-D4 (Abs. peak) under the irradiation of 620 nm at 10 cm.

620 nm 10 cm	D1	D2	D3	D4
Abs. baseline	0.003	-0.009	-0.009	0.001
0 s	0.823	1.353	0.712	0.662
1 s	0.807	1.237	0.305	0.225
2 s	0.791	1.109	0.069	0.073
3 s	0.773	0.969	0.018	0.069
4 s	0.757	0.855	0.006	0.071
5 s	0.743	0.758	0.004	0.075
10 s	0.701	0.504	0.001	0.053
15 s	0.655	0.340	0.002	0.056
30 s	0.517	0.083	0.002	0.049
60 s	0.419	0.011	0.000	0.057
120 s	0.264	0.006	0.001	-0.002
180 s	0.181	0.006	0.000	0.046
300 s	0.126	0.005	0.000	0.047
600 s	0.107	0.005	0.001	0.046
1200 s	0.100	0.005	0.001	0.046
1800 s	0.100	0.005	0.000	0.046

Table S20. Raw data of kinetic testing. Kinetics of D1-D4 (Abs. peak) under the irradiation of 620 nm at 30 cm.

620 nm 30 cm	D1	D2	D3	D4
Abs. baseline	0.000	-0.014	-0.005	-0.004
0 s	0.826	1.483	0.687	0.507
1 s	0.822	1.423	0.521	0.407
2 s	0.819	1.368	0.356	0.353
3 s	0.815	1.319	0.239	0.311
4 s	0.810	1.276	0.164	0.292
5 s	0.808	1.224	0.103	0.276
10 s	0.798	1.103	0.029	0.218
15 s	0.791	0.986	0.014	0.195
30 s	0.769	0.712	0.001	--
60 s	0.725	0.289	0.001	0.129
120 s	0.659	0.048	0.002	0.117
180 s	0.602	0.020	0.001	0.122
300 s	0.514	0.017	0.000	0.117
600 s	0.411	0.014	0.001	0.108
1200 s	0.372	0.013	0.000	0.107
1800 s	0.353	0.013	0.000	0.107

Table S21. Raw data of kinetic testing. Kinetics of D1-D4 (Abs. peak) under the irradiation of 620 nm at 50 cm.

620 nm 50 cm	D1	D2	D3	D4
Abs. baseline	0.000	0.002	-0.005	-0.008
0 s	0.819	1.440	0.691	0.463
1 s	0.814	1.419	0.557	0.415
2 s	0.812	1.383	0.474	0.372
3 s	0.811	1.365	0.404	0.341
4 s	0.809	1.344	0.338	--
5 s	0.808	1.311	0.276	0.313
10 s	0.803	1.243	0.157	0.276
15 s	0.800	1.160	0.082	0.249
30 s	0.790	1.016	0.017	0.197
60 s	0.770	0.774	0.005	0.171
120 s	0.739	0.417	0.003	0.152
180 s	0.711	0.216	0.003	0.159
300 s	0.662	0.078	0.003	0.141
600 s	0.581	0.039	0.003	0.140
1200 s	0.520	0.037	0.003	0.140
1800 s	0.474	0.038	0.003	0.141

Table S22. Raw data of kinetic testing. Kinetics of D1-D4 (Abs. peak) under the irradiation of 620 nm at 75 cm.

620 nm 75 cm	D1	D2	D3	D4
Abs. baseline	0.000	0.000	0.000	0.003
0 s	1.288	1.492	1.189	0.549
1 s	--	--	--	--
2 s	--	--	--	--
3 s	--	--	--	--
4 s	--	--	--	--
5 s	1.271	1.104	0.690	0.500
10 s	1.271	0.941	0.522	0.469
15 s	1.245	0.802	0.376	0.450
30 s	1.241	0.447	0.139	0.370
60 s	1.223	0.172	0.048	0.326
120 s	1.187	0.079	0.036	0.306
180 s	1.158	0.065	0.037	0.299
300 s	1.113	0.071	0.033	0.295
600 s	1.044	0.071	0.033	0.293
1200 s	0.978	0.061	0.033	0.288
1800 s	0.966	0.065	0.033	0.286

Table S23. Raw data of kinetic testing. Kinetics of D1-D4 (Abs. peak) under the irradiation of 620 nm at 100 cm.

620 nm 100 cm	D1	D2	D3	D4
Abs. baseline	-0.007	0.000	-0.009	0.001
0 s	0.804	1.403	0.713	0.830
1 s	0.803	1.397	0.672	0.806
2 s	0.803	1.395	0.632	0.786
3 s	0.805	1.379	0.596	0.770
4 s	0.805	1.367	0.560	0.758
5 s	0.805	1.360	0.524	0.745
10 s	0.806	1.334	0.445	0.713
15 s	0.804	1.315	0.377	0.701
30 s	0.801	1.244	0.204	0.655
60 s	0.797	1.146	0.070	0.608
120 s	0.793	0.980	0.025	0.578
180 s	0.783	0.817	0.018	0.573
300 s	0.769	0.578	0.021	0.555
600 s	0.748	0.259	0.021	0.553
1200 s	0.721	0.120	0.016	0.552
1800 s	0.711	0.107	0.019	0.552

Table S24. Raw data of kinetic testing. Kinetics of D1-D4 (Abs. peak) under the irradiation of 620 nm at 200 cm.

620 nm 200 cm	D1	D2	D3	D4
Abs. baseline	0.000	0.000	0.000	0.006
0 s	1.282	1.403	1.192	0.555
1 s	--	1.392	--	--
2 s	--	1.387	--	--
3 s	--	1.381	--	--
4 s	--	1.374	--	--
5 s	1.277	1.369	1.052	0.546
10 s	1.275	1.351	0.994	0.539
15 s	1.275	1.357	0.951	0.532
30 s	1.275	1.341	0.829	0.522
60 s	1.274	1.308	0.613	0.508
120 s	1.271	1.261	0.367	0.498
180 s	1.264	1.204	0.192	0.496
300 s	1.259	1.092	0.102	0.495
600 s	1.248	0.909	0.095	0.491
1200 s	1.235	0.621	0.095	0.489
1800 s	1.231	0.432	0.089	0.488

Table S25. Raw data of kinetic testing. Kinetics of D1-D4 (Abs. peak) under the irradiation of 660 nm at 5 cm.

660 nm 5 cm	D1	D2	D3	D4
Abs. baseline	0.000	-0.004	-0.003	0.000
0 s	0.538	1.360	0.462	1.522
1 s	0.540	1.349	0.354	0.692
2 s	0.535	1.333	0.288	0.117
3 s	0.534	1.322	0.227	0.065
4 s	0.532	1.307	0.167	0.072
5 s	0.531	1.294	0.130	0.070
10 s	0.529	1.260	0.062	0.021
15 s	0.525	1.240	0.029	0.053
30 s	0.519	1.170	0.003	0.074
60 s	0.505	1.033	0.001	0.056
120 s	0.479	0.800	0.001	0.060
180 s	0.457	0.623	0.000	0.057
300 s	0.417	0.378	0.000	0.057
600 s	0.349	0.126	0.000	0.057
1200 s	0.274	0.052	0.000	0.057
1800 s	0.244	0.048	0.000	0.057

Table S26. Raw data of kinetic testing. Kinetics of D1-D4 (Abs. peak) under the irradiation of 660 nm at 10 cm.

660 nm 10 cm	D1	D2	D3	D4
Abs. baseline	0.002	-0.002	-0.01	0.002
0 s	0.829	1.434	0.683	0.660
1 s	0.824	1.396	0.550	0.094
2 s	0.823	1.381	0.467	0.093
3 s	0.823	1.377	0.374	0.050
4 s	0.823	1.136	0.296	0.048
5 s	0.818	1.351	0.227	0.062
10 s	0.818	1.315	0.104	0.047
15 s	0.801	1.281	0.048	0.040
30 s	0.798	1.180	0.008	0.037
60 s	0.786	0.980	0.004	0.045
120 s	0.763	0.694	0.005	0.045
180 s	0.744	0.499	0.004	0.043
300 s	0.714	0.278	0.005	0.038
600 s	0.669	0.114	0.005	0.043
1200 s	0.625	0.093	0.005	0.039
1800 s	0.617	0.092	0.005	0.038

Table S27. Raw data of kinetic testing. Kinetics of D1-D4 (Abs. peak) under the irradiation of 660 nm at 30 cm.

660 nm 30 cm	D1	D2	D3	D4
Abs. baseline	-0.002	-0.014	-0.004	-0.004
0 s	0.813	1.467	0.653	0.500
1 s	0.812	1.450	0.596	0.381
2 s	0.811	1.440	0.540	0.285
3 s	0.810	1.431	0.500	0.245
4 s	0.810	1.428	0.471	0.207
5 s	0.810	1.422	0.455	0.190
10 s	0.809	1.401	0.360	0.084
15 s	0.809	1.382	0.285	0.105
30 s	0.807	1.351	0.114	0.083
60 s	0.805	1.270	0.025	0.083
120 s	0.800	1.148	0.015	0.082
180 s	0.796	1.026	0.013	--
300 s	0.788	0.831	0.014	--
600 s	0.775	0.510	0.014	0.086
1200 s	0.760	0.281	0.014	0.079
1800 s	0.755	0.221	0.014	0.079

Table S28. Raw data of kinetic testing. Kinetics of D1-D4 (Abs. peak) under the irradiation of 660 nm at 50 cm.

660 nm 50 cm	D1	D2	D3	D4
Abs. baseline	0.005	0.000	0.000	-0.008
0 s	0.815	1.445	1.198	0.462
1 s	0.814	1.443	--	0.398
2 s	0.814	1.437	--	0.352
3 s	0.813	1.440	--	0.309
4 s	0.813	1.439	--	0.277
5 s	0.813	1.434	0.925	0.261
10 s	0.812	1.428	0.812	0.215
15 s	0.812	1.423	0.691	0.169
30 s	0.812	1.411	0.441	0.142
60 s	0.812	1.377	0.177	0.127
120 s	0.811	1.300	0.085	
180 s	0.809	1.228	0.065	0.110
300 s	0.804	1.119	0.062	0.112
600 s	0.799	0.885	0.055	0.117
1200 s	0.793	0.610	0.057	0.111
1800 s	0.791	0.471	0.055	0.112

Table S29. Raw data of kinetic testing. Kinetics of D1-D4 (Abs. peak) under the irradiation of 660 nm at 75 cm.

660 nm 75 cm	D1	D2	D3	D4
Abs. baseline	0.000	-0.005	-0.004	0.003
0 s	1.271	1.352	0.462	0.547
1 s	--	1.347	0.450	--
2 s	--	1.345	0.441	--
3 s	--	1.338	0.431	--
4 s	--	1.336	0.416	--
5 s	1.271	1.331	0.404	0.462
10 s	1.271	1.325	0.375	0.409
15 s	1.271	1.321	0.355	0.366
30 s	1.270	1.314	0.205	0.297
60 s	1.268	1.306	0.218	0.249
120 s	1.267	1.288	0.138	0.223
180 s	1.264	1.261	0.090	0.219
300 s	1.260	1.211	0.048	0.211
600 s	1.254	1.083	0.024	--
1200 s	1.246	0.905	0.025	0.209
1800 s	1.243	0.774	0.024	0.210

Table S30. Raw data of kinetic testing. Kinetics of D1-D4 (Abs. peak) under the irradiation of 660 nm at 100 cm.

660 nm 100 cm	D1	D2	D3	D4
Abs. baseline	-0.001	0.003	-0.006	0.001
0 s	0.834	1.503	0.702	0.833
1 s	0.831	--	0.687	0.791
2 s	0.831	1.496	0.676	0.758
3 s	0.830	1.508	0.669	0.728
4 s	0.830	1.492	0.657	0.706
5 s	0.829	1.481	0.648	0.670
10 s	0.830	1.486	0.626	0.657
15 s	0.831	1.483	0.605	0.639
30 s	0.831	1.463	0.550	0.580
60 s	0.831	1.453	0.458	0.502
120 s	0.832	1.428	0.311	0.496
180 s	0.831	1.412	0.237	0.495
300 s	0.832	1.368	0.161	0.456
600 s	0.831	1.272	0.102	0.458
1200 s	0.829	1.142	0.081	0.456
1800 s	0.828	1.050	0.073	0.456

Table S31. Raw data of kinetic testing. Kinetics of D1-D4 (Abs. peak) under the irradiation of 660 nm at 200 cm.

660 nm 200 cm	D1	D2	D3	D4
Abs. baseline	-0.008	0.007	-0.003	0.006
0 s	0.584	1.423	0.487	0.555
1 s	0.583	1.421	0.484	--
2 s	0.583	1.417	0.481	--
3 s	0.582	1.413	0.478	--
4 s	0.582	1.412	0.476	--
5 s	0.582	1.408	0.472	0.540
10 s	0.582	1.410	0.467	0.528
15 s	0.582	1.410	0.462	0.517
30 s	0.583	1.417	0.450	0.500
60 s	0.583	1.413	0.431	0.481
120 s	0.584	1.407	0.391	0.466
180 s	0.584	1.403	0.352	0.460
300 s	0.584	1.400	0.294	0.449
600 s	0.584	1.368	0.208	0.452
1200 s	0.583	1.329	0.115	0.446
1800 s	0.582	1.284	0.088	0.445

Table S32. *linear* content (%) at PSS. Fitted *linear* content (%) at equilibrium and R-square corresponding to 28 irradiation conditions.

	linear content (%)/R-square							
Conditions	D1		D2		D3		D4	
dark	100.00	-	100.00	-	100.00	-	100.00	-
520 nm 5 cm	0.55	0.999	0.31	0.994	0.57	0.997	18.84	0.996
520 nm 10 cm	0.46	0.993	0.89	0.711	1.83	0.999	67.91	0.930
520 nm 30 cm	2.18	0.996	1.37	0.999	4.56	0.998	82.56	0.974
520 nm 50 cm	5.55	0.999	2.08	0.999	7.72	0.999	92.01	0.959
520 nm 75 cm	13.21	0.995	4.01	0.993	11.52	0.998	96.47	0.989
520 nm 100 cm	20.28	0.999	6.04	0.998	22.13	0.999	96.63	0.966
520 nm 200 cm	34.46	0.999	10.11	0.999	40.90	0.997	99.25	0.747
590 nm 5 cm	1.83	0.995	0.02	0.997	0.00	0.997	17.70	0.988
590 nm 10 cm	3.19	0.995	0.06	0.989	1.16	0.997	26.20	0.968
590 nm 30 cm	8.16	0.998	0.29	0.999	2.67	0.995	57.20	0.980
590 nm 50 cm	14.20	0.999	0.30	0.999	3.21	0.995	72.30	0.984
590 nm75 cm	26.58	0.998	0.46	0.999	4.59	0.996	83.44	0.979
590 nm 100 cm	36.79	0.998	0.50	0.998	7.34	0.998	89.40	0.977
590 nm 200 cm	53.44	0.998	6.09	0.998	9.85	0.999	96.45	0.916
620 nm 5 cm	8.77	0.975	1.12	0.994	0.00	0.999	15.14	0.991
620 nm 10 cm	13.24	0.996	1.39	0.998	0.93	0.995	16.63	0.996
620 nm 30 cm	43.44	0.999	1.52	0.999	0.89	0.998	24.41	0.974
620 nm 50 cm	57.77	0.997	2.33	0.999	1.78	0.997	33.92	0.975
620 nm 75 cm	74.89	0.994	4.66	0.997	3.25	0.995	53.27	0.996
620 nm 100 cm	87.31	0.998	6.89	0.999	4.11	0.998	67.66	0.983
620 nm 200 cm	95.78	0.990	13.11	0.998	7.38	0.997	88.51	0.990
660 nm 5 cm	42.37	0.999	3.63	0.999	1.31	0.998	3.12	0.986
660 nm10 cm	74.39	0.994	6.26	0.988	2.37	0.999	6.81	0.993
660 nm 30 cm	92.49	0.998	14.49	0.999	2.70	0.997	17.41	0.994
660 nm 50 cm	96.77	0.989	23.18	0.999	5.15	0.998	27.44	0.987
660 nm 75 cm	97.79	-	30.75	0.998	9.65	0.975	39.31	0.996
660 nm 100 cm	99.33	-	61.66	0.996	13.18	0.998	56.70	0.965
660 nm 200 cm	99.81	0.112	99.67	0.956	17.04	0.999	81.01	0.956

9. Concentration-dependence of D1-D4

DASAs are negative photochromic molecules switching from colored to colorless under exposing to light. This improves the penetration of light into the sample during the photoisomerization. Previous research reported the isomerization of DASAs is interrelated with the concentration. In the solutions with high concentration, neighboring molecules interact electronically and form delocalized excited states (excitons) with different reactivities. Steric interactions prevent the nuclear motions necessary for the isomerization. Therefore, the photoisomerization of DASAs is limited with the increase of concentration.

The concentration-dependence of DASAs is important for the simulation of color accuracy of SAP materials under light irradiation. The kinetics for the light-induced *linear*-to-*cyclic* isomerization of DASA solutions with the initial absorbance of 1, 6 and 25 (the corresponding concentrations are 3.2×10^{-5} M, 1.9×10^{-4} M and 8.2×10^{-4} M, respectively) were studied. A cuvette with the optical path of 1 mm was used for the measurement of the DASA solutions with the initial absorbance of 6 and 25 (A=0.6 and 2.5).

For all the DASAs, the concentration-dependence is not that obvious. Actually, increasing the concentration results in slightly higher *linear* content at equilibrium in some cases (**Fig. S18**). These might be attributed to the narrowly-distributed concentration of DASA solutions, which is much lower than the previous research (1×10^{-2} M). Therefore, under the same irradiation condition, the DASA solutions with the initial absorbance ranged between 1 and 25 show similar *linear* content at equilibrium.

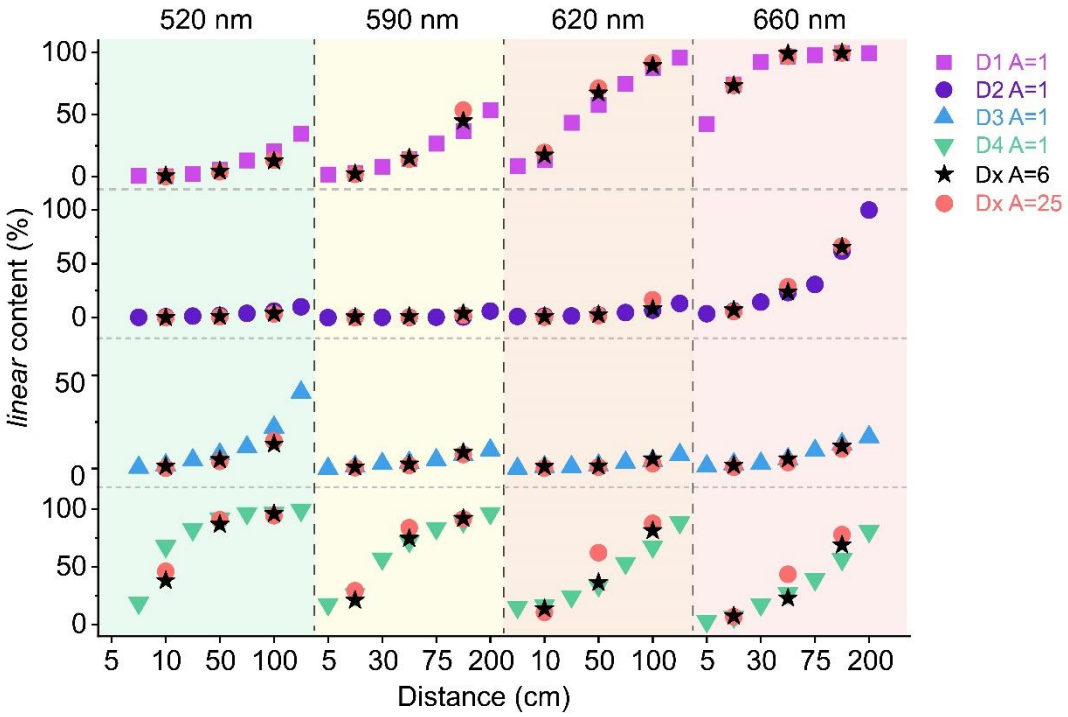

Fig. S18. Equilibrium *linear* content (%) at different concentrations. Equilibrium *linear* content (%) of DASA (D1-D4) solutions with the initial absorbance at 1, 6 and 25 under light irradiation.

10. Optimization of SAP materials

Table S33. Concentration coefficients of different strategies. The concentration of color-contributing units of A2, A4, A6, A8, R6 and R8.

Mode	Concentration (μM)							
	a	b	c	d	e	f	g	h
A2	0.00	0.00	0.00	20.02	0.00	0.00	0.00	13.01
A4	36.08	0.00	15.81	0.00	37.24	0.00	0.00	13.01
A6	36.08	38.52	15.81	0.00	37.24	29.89	0.00	13.01
A8	36.08	38.52	15.81	20.02	37.24	29.89	25.30	13.01
R6	28.86	38.52	9.48	0.00	29.80	19.43	0.00	15.61
R8	41.49	63.56	4.74	33.03	50.28	23.91	20.24	24.72

Table S34. Color coordinates of different strategies. *L**, *a**, *b** values of A2, A4, A6, A8, R6 and R8.

Spectra Label	L*	a*	b*
A2	74.89535	-10.1044	19.35718
A4	57.03506	-4.40115	4.61268
A6	54.62911	-20.8554	11.15192
A8	48.82071	-9.5412	8.76253
R6	52.80483	-33.9646	8.34636
R8	41.77479	-3.06623	4.28341

Table S35. Color coordinates of A4 strategy at different concentrations. *L**, *a**, *b** values of A4 solutions with the initial absorbance between 0.5 and 50.

Maximum Abs.	*a**	*b**	*L**
A=0.5	75.07314	-2.12194	3.15197
A=1	57.03506	-4.40115	4.61268
A=2	33.54306	-7.48394	4.48618
A=4	10.35173	-4.26569	1.57458
A=6	2.48391	3.21932	0.47888
A=8	0.97248	4.50548	0.62926
A=10	0.60011	4.21131	0.71325
A=25	0.22328	1.84109	0.38476
A=50	0.08981	0.74071	0.15485

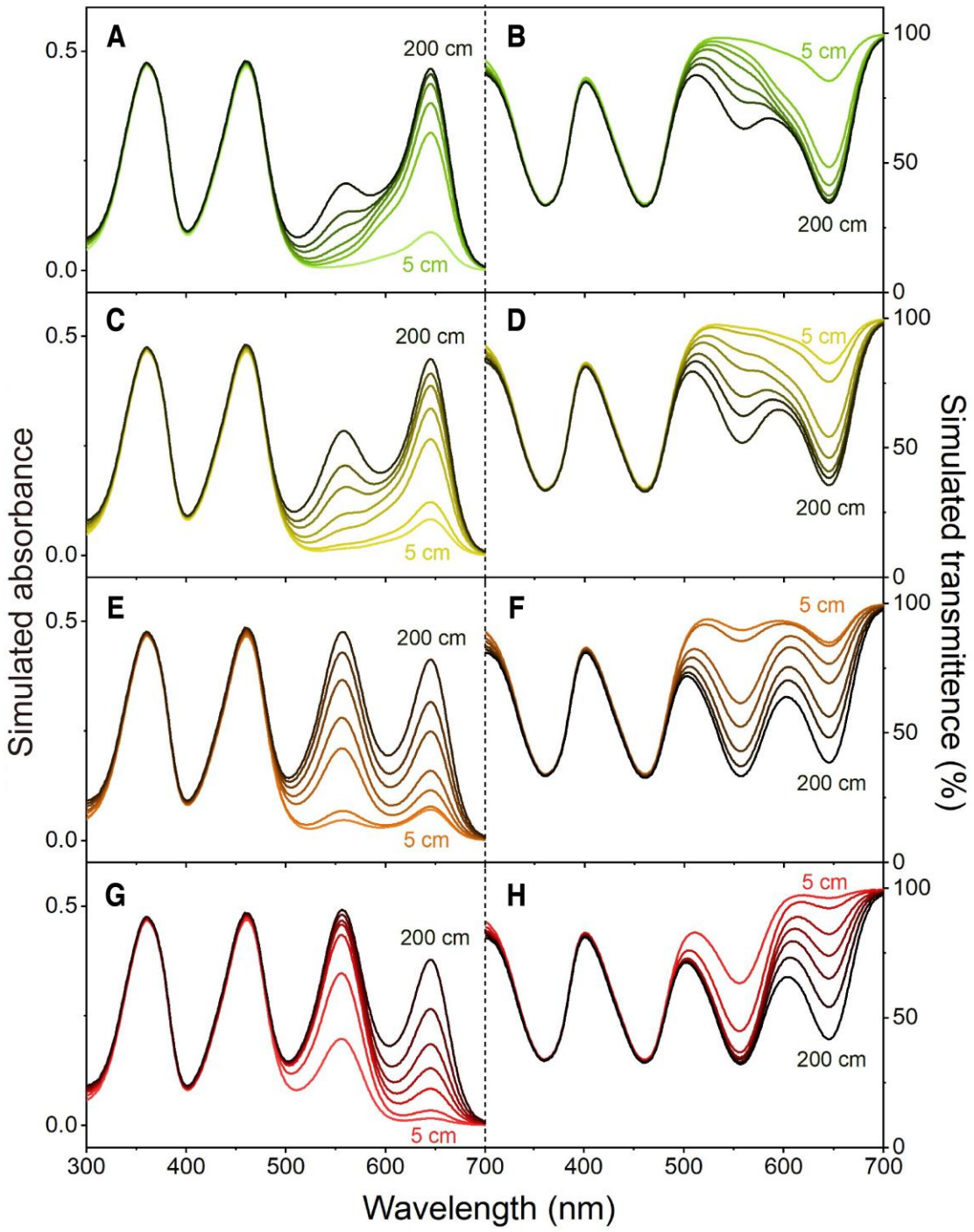

Fig. S19. Absorption/transmission spectra with an initial absorbance of 0.5 under different light conditions. Simulated absorption (left) and transmission (right) spectra of A4 solution (initial absorbance=0.5) under 520 (**A** and **B**), 590 (**C** and **D**), 620 (**E** and **F**) and 660 nm (**G** and **H**) irradiation at different distances.

Table S36. Color coordinates with an initial absorbance of 0.5 under different light conditions. *L**, *a**, *b** values of A4 solution (initial absorbance=0.5) under light irradiation.

A=0.5	*L**	*a**	*b**
dark	75.07314	-2.12194	3.15197
520 nm 5 cm	97.0253	-15.56462	36.89632
520 nm 10 cm	93.96224	-26.47936	32.26933
520 nm 30 cm	92.77143	-28.76103	30.46895
520 nm 50 cm	91.55772	-29.3839	28.61403
520 nm 75 cm	89.77196	-27.61884	25.84587
520 nm 100 cm	88.37894	-25.30132	23.67483
520 nm 200 cm	85.57901	-21.19652	19.33071
590 nm 5 cm	96.83911	-14.82592	36.6029
590 nm 10 cm	95.98795	-16.38304	35.29506
590 nm 30 cm	93.01601	-21.58228	30.75093
590 nm 50 cm	90.92026	-22.63326	27.53673
590 nm75 cm	87.90366	-20.72631	22.88139
590 nm 100 cm	85.69352	-18.59274	19.47025
590 nm 200 cm	82.40494	-14.76511	14.40246
620 nm 5 cm	95.61002	-11.72009	34.68013
620 nm 10 cm	94.62386	-10.51759	33.14667
620 nm 30 cm	88.53384	-2.32138	23.70789
620 nm 50 cm	85.48357	-0.12288	19.01022
620 nm 75 cm	81.51561	0.52756	12.93028
620 nm 100 cm	78.76583	0.92795	8.73598
620 nm 200 cm	76.31358	-1.0247	5.02179
660 nm 5 cm	90.24188	2.74223	26.33472
660 nm10 cm	84.82114	11.63384	17.99585
660 nm 30 cm	81.41398	14.04873	12.7803
660 nm 50 cm	80.09337	12.72692	10.75699
660 nm 75 cm	79.12285	10.15916	9.27001
660 nm 100 cm	77.75584	6.60946	7.18671
660 nm 200 cm	76.1881	1.57348	4.81863

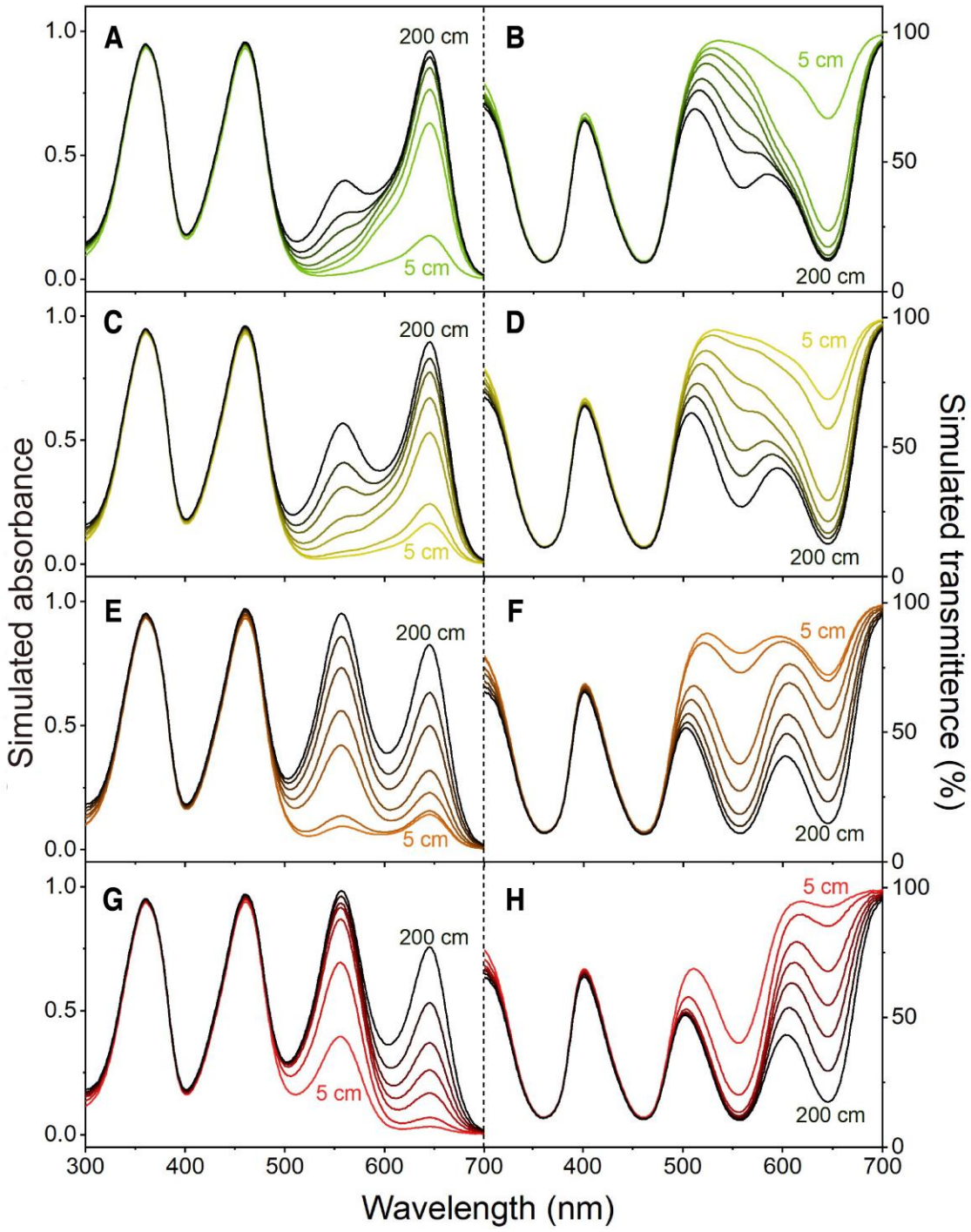

Fig. S20. Absorption/transmission spectra with an initial absorbance of 1 under different light conditions. Simulated absorption (left) and transmission (right) spectra of A4 solution (initial absorbance=1) under 520 (**A** and **B**), 590 (**C** and **D**), 620 (**E** and **F**) and 660 nm (**G** and **H**) irradiation at different distances.

Table S37. Color coordinates with an initial absorbance of 1 under different light conditions. *L**, *a**, *b** values of A4 solution (initial absorbance=1) under light irradiation.

A=1	*L**	*a**	*b**
dark	57.03506	-4.40115	4.61268
520 nm 5 cm	94.65263	-24.4311	61.83168
520 nm 10 cm	89.18533	-44.30581	53.43916
520 nm 30 cm	87.09005	-47.93555	50.26089
520 nm 50 cm	84.86929	-48.69153	46.87457
520 nm 75 cm	81.46732	-45.43656	41.64382
520 nm 100 cm	78.81972	-41.41663	37.56469
520 nm 200 cm	73.73675	-34.38644	29.77546
590 nm 5 cm	94.26917	-22.99731	61.24147
590 nm 10 cm	92.62597	-26.06445	58.69034
590 nm 30 cm	87.10221	-35.60965	50.18338
590 nm 50 cm	83.25402	-37.26331	44.28999
590 nm75 cm	77.74089	-33.77146	35.84809
590 nm 100 cm	73.82913	-30.0953	29.87733
590 nm 200 cm	68.25243	-23.78045	21.40736
620 nm 5 cm	91.82399	-17.02265	57.47678
620 nm 10 cm	89.91465	-14.81275	54.53296
620 nm 30 cm	78.83804	-0.57085	37.56708
620 nm 50 cm	73.62565	2.39678	29.62408
620 nm 75 cm	67.06282	2.02927	19.6581
620 nm 100 cm	62.72742	1.69531	13.12966
620 nm 200 cm	58.90555	-2.31886	7.39502
660 nm 5 cm	82.22588	9.97279	42.89282
660 nm10 cm	73.53113	23.93071	29.81149
660 nm 30 cm	68.13491	25.95726	21.66951
660 nm 50 cm	65.82836	22.69403	18.11595
660 nm 75 cm	63.99806	17.61047	15.25817
660 nm 100 cm	61.54286	10.82369	11.46168
660 nm 200 cm	58.83499	1.84641	7.31772

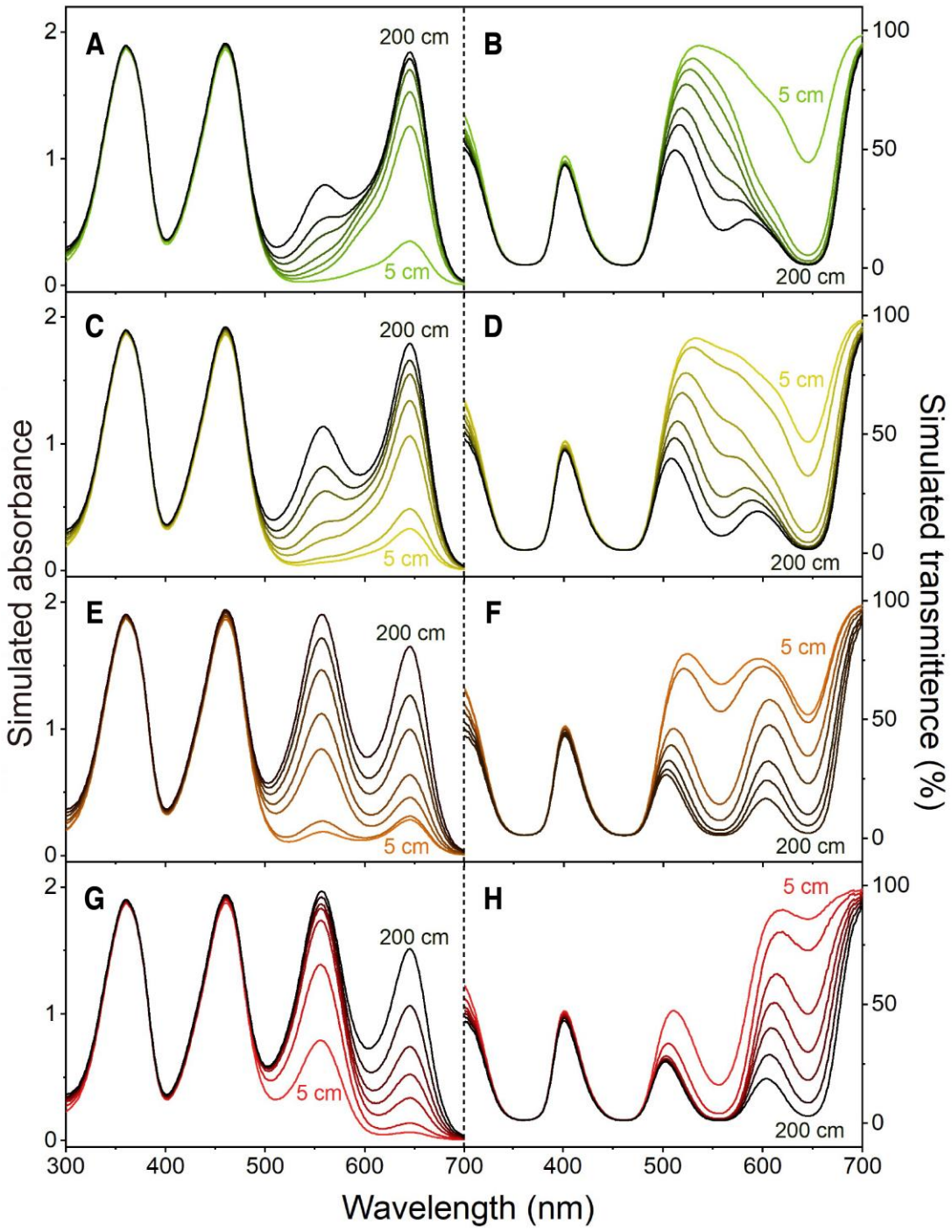

Fig. S21. Absorption/transmission spectra with an initial absorbance of 2 under different light conditions. Simulated absorption (left) and transmission (right) spectra of A4 solution (initial absorbance=2) under 520 (**A** and **B**), 590 (**C** and **D**), 620 (**E** and **F**) and 660 nm (**G** and **H**) irradiation at different distances.

Table S38. Color coordinates with an initial absorbance of 2 under different light conditions. *L**, *a**, *b** values of A4 solution (initial absorbance=2) under light irradiation.

A=2	*L**	*a**	*b**
dark	33.54306	-7.48394	4.48618
520 nm 5 cm	90.76922	-34.07951	88.95433
520 nm 10 cm	81.83773	-65.44605	74.95567
520 nm 30 cm	78.40418	-69.79281	69.76876
520 nm 50 cm	74.54547	-69.9798	63.98675
520 nm 75 cm	68.40643	-64.46689	54.82248
520 nm 100 cm	63.73161	-58.30274	47.8722
520 nm 200 cm	55.44656	-47.70167	35.64644
590 nm 5 cm	89.96959	-31.40048	87.78674
590 nm 10 cm	86.91632	-36.8289	83.02727
590 nm 30 cm	77.27438	-51.754	68.18295
590 nm 50 cm	70.69431	-53.40563	58.26899
590 nm75 cm	61.47423	-47.34497	44.54661
590 nm 100 cm	55.35045	-41.66134	35.52191
590 nm 200 cm	47.29282	-32.55711	23.79358
620 nm 5 cm	85.17738	-20.23848	80.71294
620 nm 10 cm	81.62667	-16.2802	75.39524
620 nm 30 cm	63.3017	6.25317	48.30082
620 nm 50 cm	55.5609	8.7468	36.84844
620 nm 75 cm	46.27653	5.00647	23.07128
620 nm 100 cm	40.62114	2.6167	14.80844
620 nm 200 cm	35.76732	-4.25507	7.68793
660 nm 5 cm	69.98155	26.94333	59.09042
660 nm10 cm	58.58558	43.52817	42.97709
660 nm 30 cm	51.06499	41.36292	31.88803
660 nm 50 cm	47.21951	34.51791	25.87861
660 nm 75 cm	43.93175	25.83226	20.61401
660 nm 100 cm	39.91541	14.76763	14.27848
660 nm 200 cm	35.88793	1.2985	8.01722

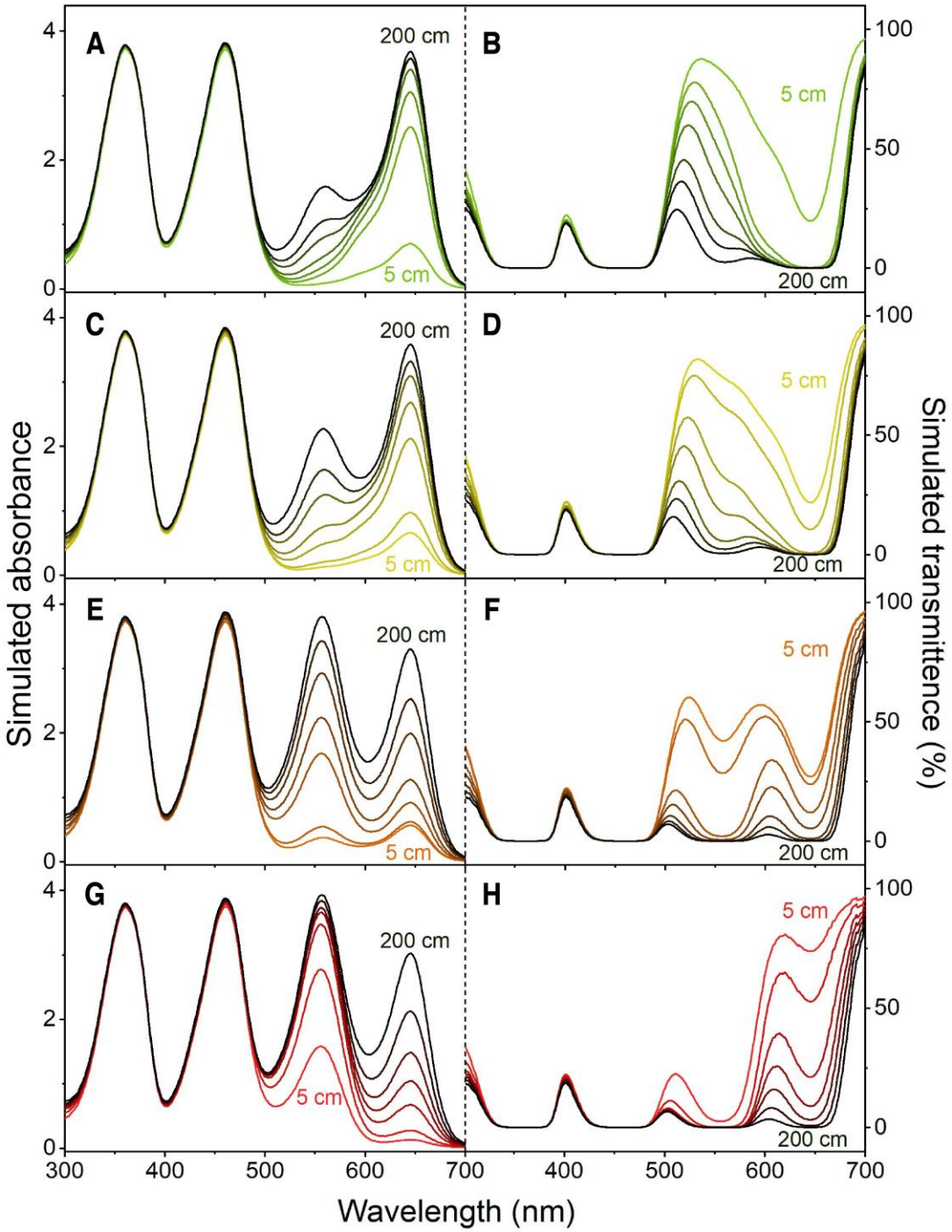

Fig. S22. Absorption/transmission spectra with an initial absorbance of 4 under different light conditions. Simulated absorption (left) and transmission (right) spectra of A4 solution (initial absorbance=4) under 520 (**A** and **B**), 590 (**C** and **D**), 620 (**E** and **F**) and 660 nm (**G** and **H**) irradiation at different distances.

Table S39. Color coordinates with an initial absorbance of 4 under different light conditions. *L**, *a**, *b** values of A4 solution (initial absorbance=4) under light irradiation.

A=4	*L**	*a**	*b**
dark	10.35173	-4.26569	1.57458
520 nm 5 cm	84.53756	-44.36714	104.50689
520 nm 10 cm	71.53315	-82.94092	83.91686
520 nm 30 cm	66.25988	-85.64412	76.17549
520 nm 50 cm	60.00699	-83.7149	67.23499
520 nm 75 cm	50.08905	-75.18851	53.33627
520 nm 100 cm	43.03324	-66.93844	43.60615
520 nm 200 cm	32.07899	-52.76493	28.7953
590 nm 5 cm	82.85833	-39.68888	102.22184
590 nm 10 cm	77.53968	-47.47474	94.05834
590 nm 30 cm	62.23115	-64.6067	71.02492
590 nm 50 cm	52.23564	-64.10813	56.65627
590 nm75 cm	39.2022	-54.23326	38.53466
590 nm 100 cm	31.57958	-46.10789	28.23431
590 nm 200 cm	22.77055	-33.71992	16.7154
620 nm 5 cm	73.78204	-19.91748	89.71332
620 nm 10 cm	67.69332	-13.13175	81.10233
620 nm 30 cm	42.06968	16.92728	45.99474
620 nm 50 cm	32.75679	16.39767	32.99184
620 nm 75 cm	22.22198	8.37611	17.96312
620 nm 100 cm	16.58247	4.64911	10.14864
620 nm 200 cm	12.14021	-1.93332	3.94417
660 nm 5 cm	54.967	51.23757	67.3319
660 nm10 cm	43.45168	60.31011	53.15164
660 nm 30 cm	33.30154	49.6715	38.11346
660 nm 50 cm	27.25942	39.36191	28.42505
660 nm 75 cm	22.13726	28.69148	20.03483
660 nm 100 cm	16.76142	16.3651	11.40088
660 nm 200 cm	12.34298	3.19616	4.48811

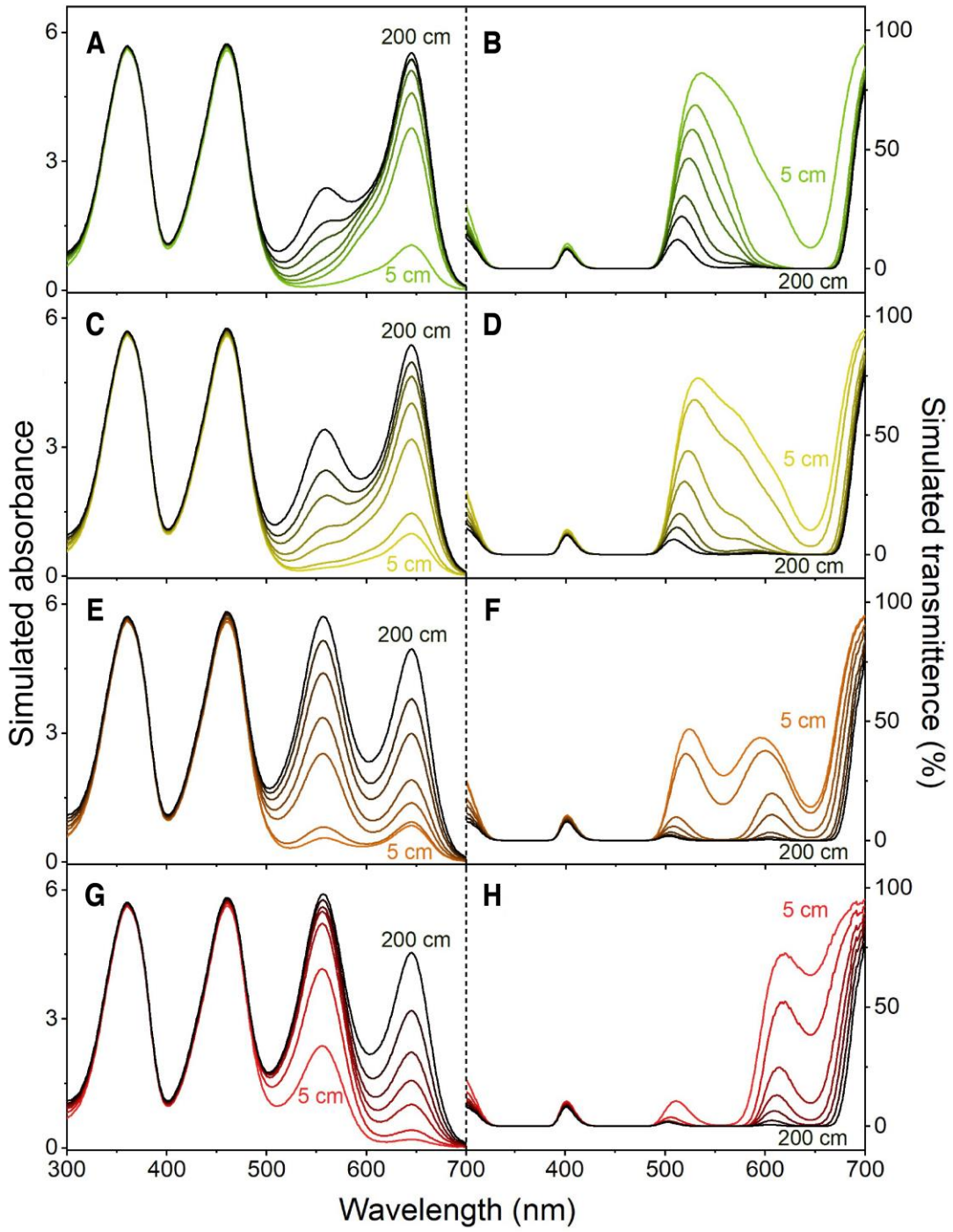

Fig. S23. Absorption/transmission spectra with an initial absorbance of 6 under different light conditions. Simulated absorption (left) and transmission (right) spectra of A4 solution (initial absorbance=6) under 520 (**A** and **B**), 590 (**C** and **D**), 620 (**E** and **F**) and 660 nm (**G** and **H**) irradiation at different distances.

Table S40. Color coordinates with an initial absorbance of 6 under different light conditions. *L**, *a**, *b** values of A4 solution (initial absorbance=6) under light irradiation.

A=6	*L**	*a**	*b**
dark	2.48391	3.21932	0.47888
520 nm 5 cm	79.38411	-51.07352	105.909
520 nm 10 cm	64.01422	-88.23282	81.76142
520 nm 30 cm	57.41187	-88.59203	72.34982
520 nm 50 cm	49.5113	-84.4614	61.47075
520 nm 75 cm	37.45775	-73.37139	45.38754
520 nm 100 cm	29.49242	-63.48118	35.08134
520 nm 200 cm	18.35927	-45.70565	20.97242
590 nm 5 cm	76.80747	-44.8878	102.49417
590 nm 10 cm	69.74517	-53.14541	91.84855
590 nm 30 cm	50.82315	-67.75254	64.09349
590 nm 50 cm	39.10699	-64.40504	47.95853
590 nm75 cm	25.02679	-50.83763	29.58944
590 nm 100 cm	17.63592	-39.88707	20.10997
590 nm 200 cm	9.83881	-21.31425	9.83134
620 nm 5 cm	64.01041	-18.41306	85.48357
620 nm 10 cm	56.18984	-9.56219	74.8485
620 nm 30 cm	28.35704	21.52608	38.69787
620 nm 50 cm	19.09173	18.82368	25.31946
620 nm 75 cm	9.20514	11.05362	10.24575
620 nm 100 cm	5.05326	7.45039	4.0259
620 nm 200 cm	3.04438	3.81566	1.17242
660 nm 5 cm	46.57525	62.19121	69.29298
660 nm10 cm	35.48719	62.50632	54.7742
660 nm 30 cm	23.25381	46.88323	34.99092
660 nm 50 cm	16.05145	35.94613	22.90965
660 nm 75 cm	10.33315	26.50086	13.24925
660 nm 100 cm	5.41187	15.87302	5.03555
660 nm 200 cm	3.11215	5.8879	1.35912

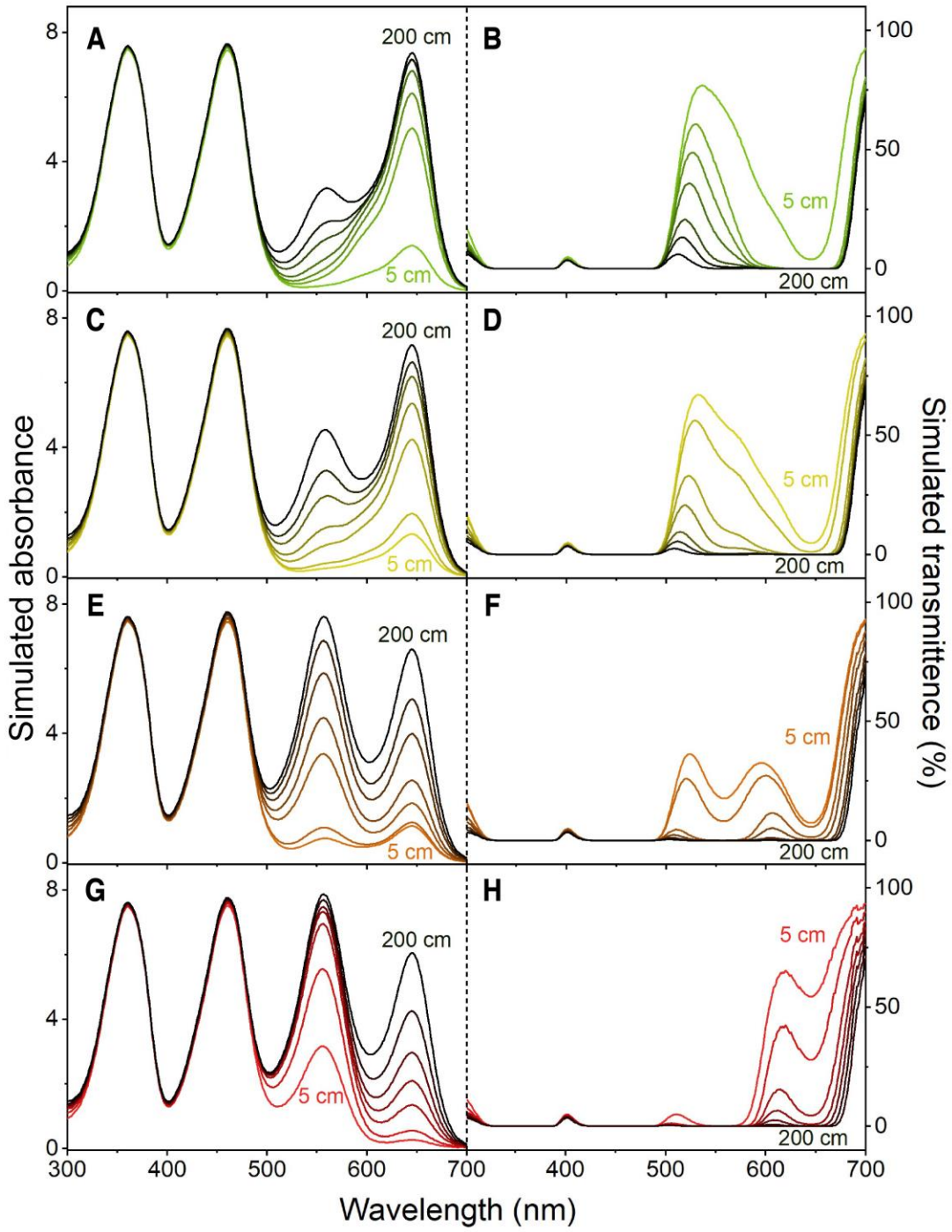

Fig. S24. Absorption/transmission spectra with an initial absorbance of 8 under different light conditions. Simulated absorption (left) and transmission (right) spectra of A4 solution (initial absorbance=8) under 520 (**A** and **B**), 590 (**C** and **D**), 620 (**E** and **F**) and 660 nm (**G** and **H**) irradiation at different distances.

Table S41. Color coordinates with an initial absorbance of 8 under different light conditions. *L**, *a**, *b** values of A4 solution (initial absorbance=8) under light irradiation.

A=8	*L**	*a**	*b**
dark	0.97248	4.50548	0.62926
520 nm 5 cm	74.92507	-55.83517	104.02919
520 nm 10 cm	57.95656	-88.85889	77.69512
520 nm 30 cm	50.32491	-87.04041	67.07541
520 nm 50 cm	41.28309	-80.8209	54.98215
520 nm 75 cm	28.13932	-66.94581	37.85496
520 nm 100 cm	20.03931	-54.79803	26.95607
520 nm 200 cm	9.6315	-26.8564	12.36842
590 nm 5 cm	71.46634	-48.4878	99.4856
590 nm 10 cm	63.02139	-56.25623	86.94902
590 nm 30 cm	41.75696	-66.76855	56.45259
590 nm 50 cm	29.32685	-60.30446	39.7325
590 nm75 cm	15.50136	-41.22305	20.7435
590 nm 100 cm	8.86097	-22.66024	11.27932
590 nm 200 cm	3.59663	-4.77306	3.84114
620 nm 5 cm	55.49107	-16.78616	78.66372
620 nm 10 cm	46.55231	-6.48636	66.84677
620 nm 30 cm	18.86094	22.90868	28.68406
620 nm 50 cm	10.20982	19.45706	15.06666
620 nm 75 cm	3.25088	9.36543	3.90281
620 nm 100 cm	1.76779	6.52311	1.6936
620 nm 200 cm	1.14145	4.89756	0.82787
660 nm 5 cm	41.21424	65.96748	66.77694
660 nm10 cm	30.01994	60.15766	49.71381
660 nm 30 cm	16.32052	41.7544	26.60052
660 nm 50 cm	8.79497	31.36515	13.75171
660 nm 75 cm	4.18827	20.42745	5.88641
660 nm 100 cm	1.96301	9.66989	2.15189
660 nm 200 cm	1.17242	5.63655	0.89819

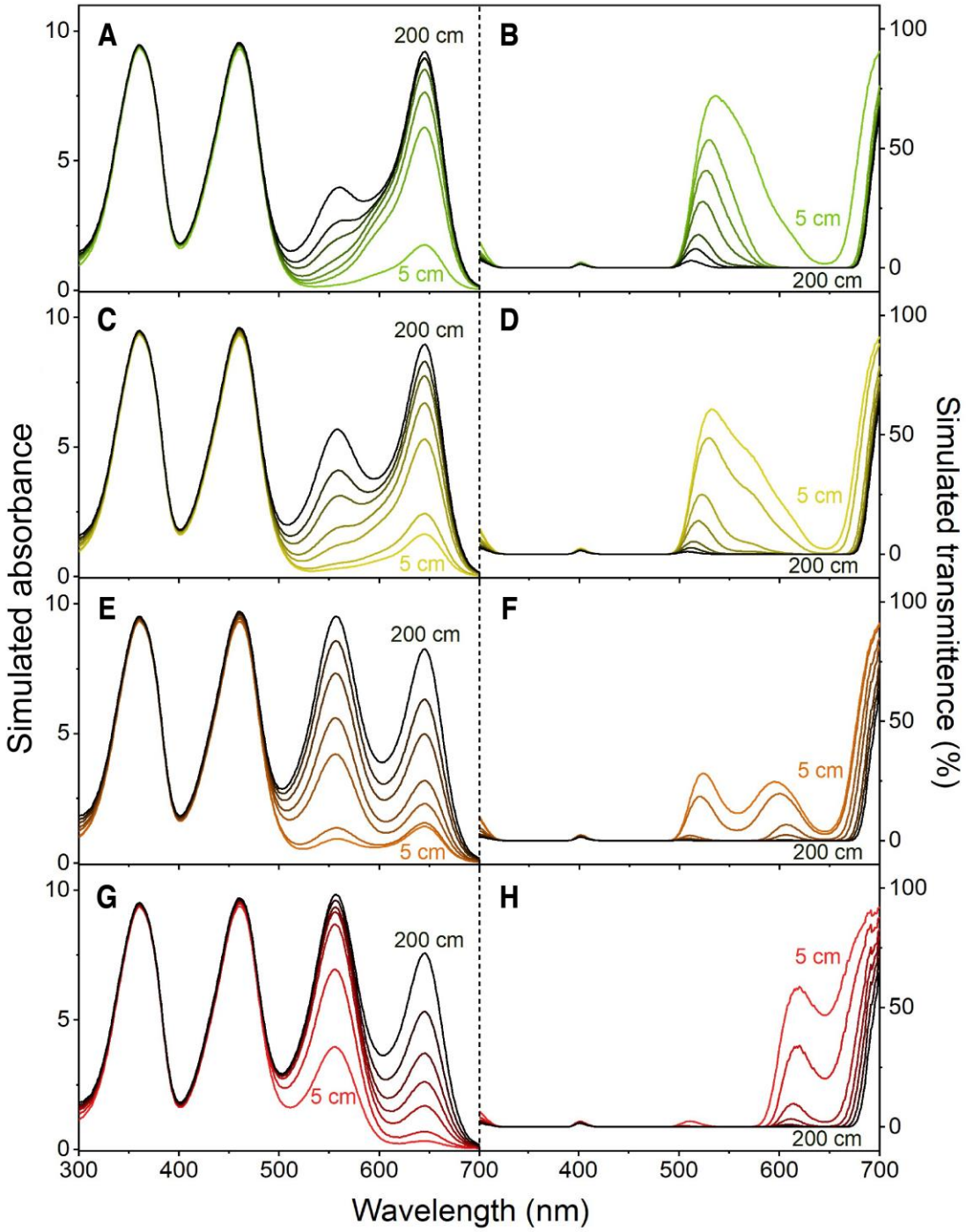

Fig. S25. Absorption/transmission spectra with an initial absorbance of 10 under different light conditions. Simulated absorption (left) and transmission (right) spectra of A4 solution (initial absorbance=10) under 520 (**A** and **B**), 590 (**C** and **D**), 620 (**E** and **F**) and 660 nm (**G** and **H**) irradiation at different distances.

Table S42. Color coordinates with an initial absorbance of 10 under different light conditions. *L**, *a**, *b** values of A4 solution (initial absorbance=10) under light irradiation.

A=10	*L**	*a**	*b**
dark	0.60011	4.21131	0.71325
520 nm 5 cm	70.9727	-59.20033	101.19167
520 nm 10 cm	52.82014	-87.39305	73.38171
520 nm 30 cm	44.37799	-83.65173	61.86281
520 nm 50 cm	34.5584	-75.46612	48.78841
520 nm 75 cm	20.9737	-58.50028	30.04624
520 nm 100 cm	13.12021	-39.67296	18.72925
520 nm 200 cm	4.45564	-10.05305	5.89183
590 nm 5 cm	66.66583	-50.93493	95.54814
590 nm 10 cm	57.10657	-57.72572	81.53774
590 nm 30 cm	34.36302	-63.62291	49.16672
590 nm 50 cm	21.81652	-53.83036	31.40995
590 nm75 cm	8.80855	-24.16171	12.36727
590 nm 100 cm	3.99936	-7.62224	5.24348
590 nm 200 cm	1.57219	0.96101	1.88108
620 nm 5 cm	48.01511	-15.1456	71.37602
620 nm 10 cm	38.42029	-3.86908	58.11368
620 nm 30 cm	12.0099	22.91469	19.17355
620 nm 50 cm	4.83162	17.3407	7.42774
620 nm 75 cm	1.49247	7.28912	2.01576
620 nm 100 cm	0.92403	5.65536	1.16308
620 nm 200 cm	0.67488	4.57242	0.80979
660 nm 5 cm	37.32402	66.39484	62.5626
660 nm10 cm	25.71302	56.55098	43.61563
660 nm 30 cm	11.13483	36.74537	18.68163
660 nm 50 cm	4.54199	24.60673	7.3643
660 nm 75 cm	2.03901	12.36483	3.08033
660 nm 100 cm	1.03629	7.00981	1.3918
660 nm 200 cm	0.70157	4.94228	0.85836

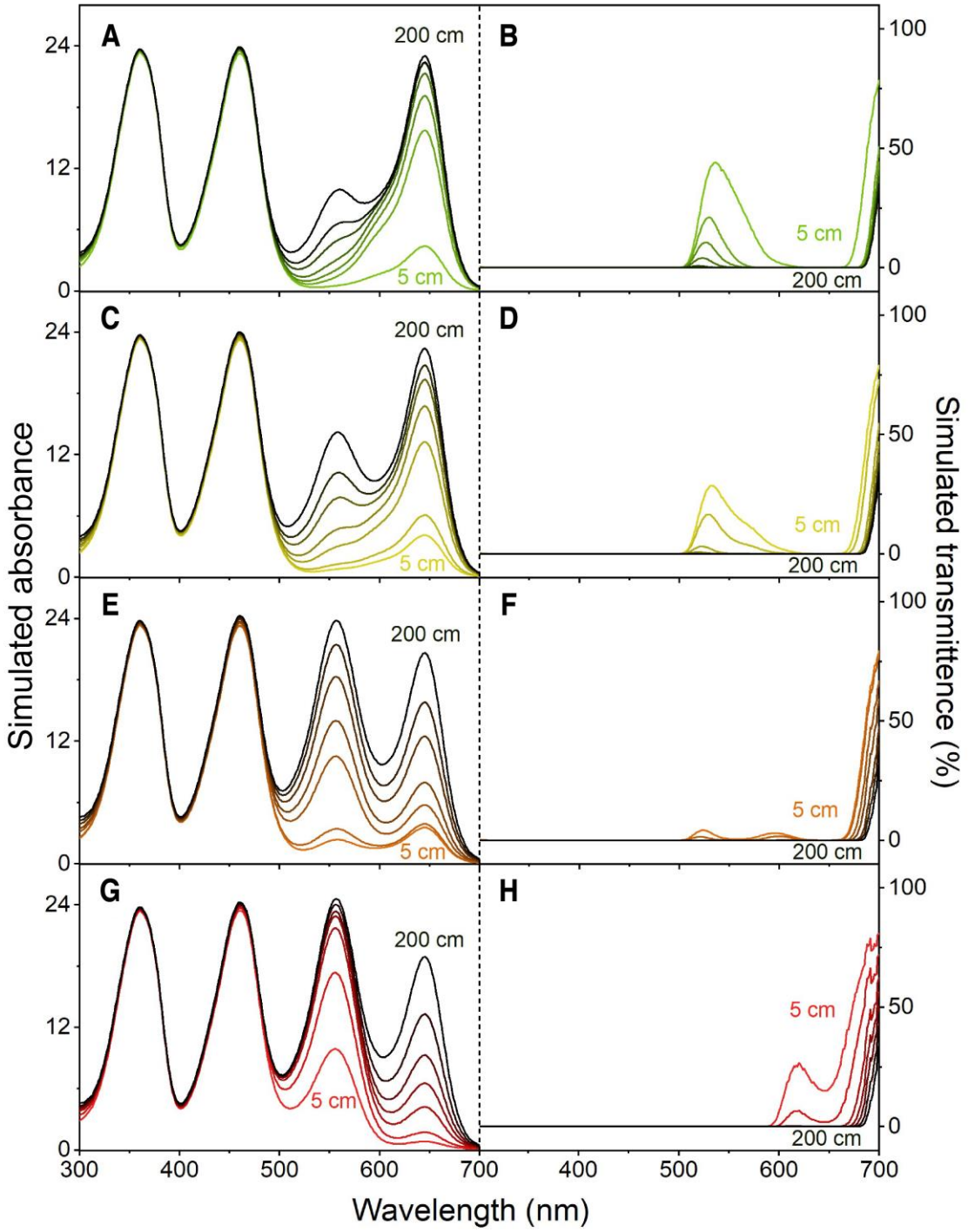

Fig. S26. Absorption/transmission spectra with an initial absorbance of 25 under different light conditions. Simulated absorption (left) and transmission (right) spectra of A4 solution (initial absorbance=25) under 520 (**A** and **B**), 590 (**C** and **D**), 620 (**E** and **F**) and 660 nm (**G** and **H**) irradiation at different distances.

Table S43. Color coordinates with an initial absorbance of 25 under different light conditions. *L**, *a**, *b** values of A4 solution (initial absorbance=25) under light irradiation.

A=25	*L**	*a**	*b**
dark	0.22328	1.84109	0.38476
520 nm 5 cm	49.96496	-63.54714	78.39018
520 nm 10 cm	27.87279	-64.24431	44.0028
520 nm 30 cm	17.18625	-49.86413	27.42332
520 nm 50 cm	6.8627	-20.60989	10.91825
520 nm 75 cm	1.17565	-0.7959	1.8456
520 nm 100 cm	0.48106	1.73367	0.77954
520 nm 200 cm	0.29108	2.24947	0.49669
590 nm 5 cm	40.85165	-51.5909	64.971
590 nm 10 cm	27.66633	-48.52457	44.34587
590 nm 30 cm	5.5438	-14.36953	8.8319
590 nm 50 cm	1.26317	-0.34112	1.9939
590 nm75 cm	0.38053	2.42077	0.6369
590 nm 100 cm	0.30592	2.41374	0.52346
590 nm 200 cm	0.2676	2.19903	0.46077
620 nm 5 cm	13.58814	-3.16375	22.44457
620 nm 10 cm	5.83603	8.07242	9.69324
620 nm 30 cm	0.80536	6.16685	1.38565
620 nm 50 cm	0.53956	4.40853	0.92946
620 nm 75 cm	0.37095	3.05625	0.63916
620 nm 100 cm	0.30343	2.50115	0.52284
620 nm 200 cm	0.24616	2.02957	0.42417
660 nm 5 cm	20.87877	52.30086	35.97161
660 nm10 cm	6.88342	33.83856	11.8629
660 nm 30 cm	0.94835	7.21164	1.63435
660 nm 50 cm	0.55403	4.51645	0.95474
660 nm 75 cm	0.42259	3.47821	0.7282
660 nm 100 cm	0.32834	2.70602	0.56578
660 nm 200 cm	0.25797	2.12684	0.44452

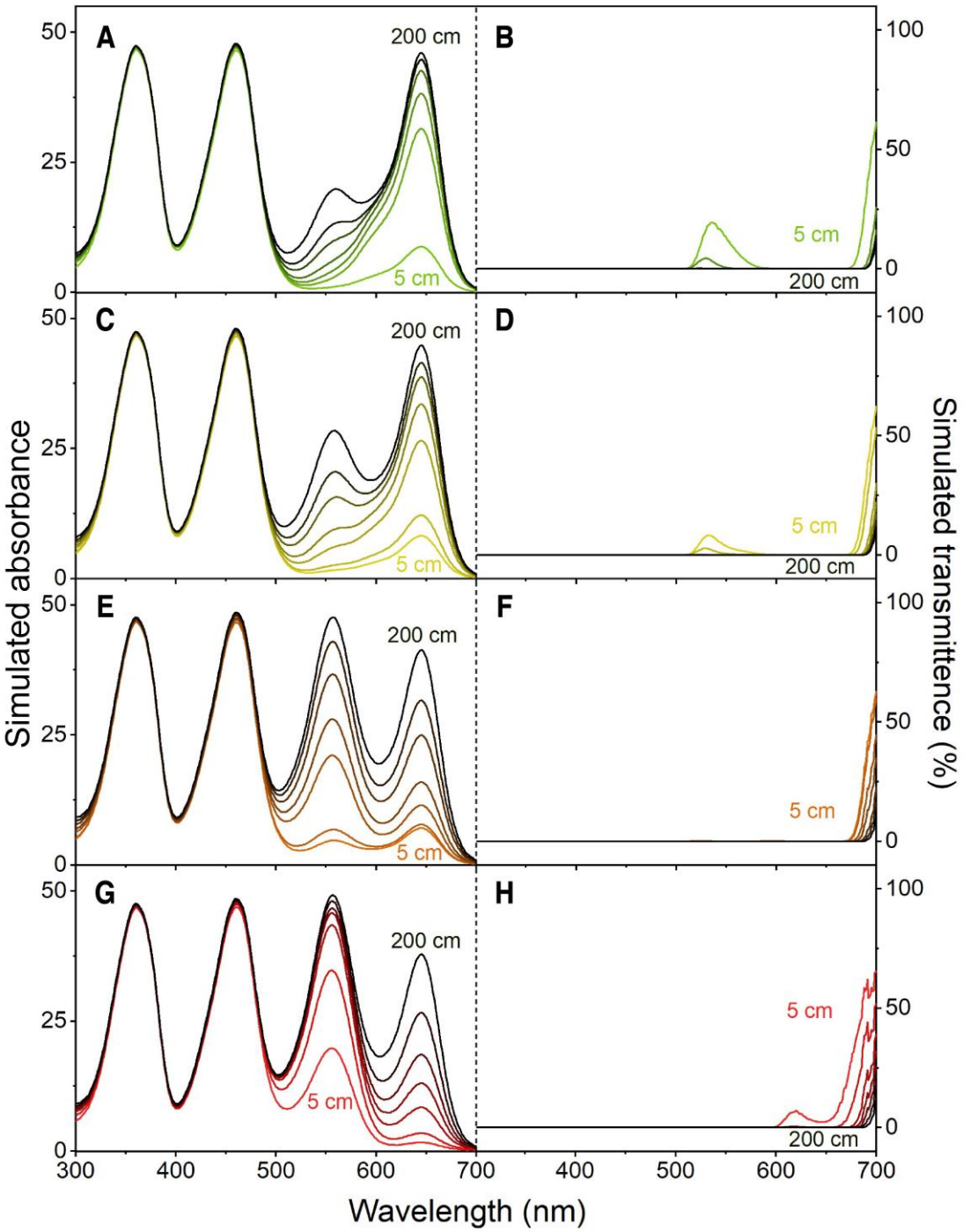

Fig. S27. Absorption/transmission spectra with an initial absorbance of 50 under different light conditions. Simulated absorption (left) and transmission (right) spectra of A4 solution (initial absorbance=50) under 520 (**A** and **B**), 590 (**C** and **D**), 620 (**E** and **F**) and 660 nm (**G** and **H**) irradiation at different distances.

Table S44. Color coordinates with an initial absorbance of 50 under different light conditions. *L**, *a**, *b** values of A4 solution (initial absorbance=50) under light irradiation.

A=50	*L**	*a**	*b**
dark	0.08981	0.74071	0.15485
520 nm 5 cm	29.328	-50.45732	48.21405
520 nm 10 cm	7.39445	-21.80926	12.16421
520 nm 30 cm	7.39445	-21.80926	12.16421
520 nm 50 cm	0.36585	0.80821	0.60516
520 nm 75 cm	0.16973	1.34687	0.29175
520 nm 100 cm	0.15766	1.29741	0.27177
520 nm 200 cm	0.14013	1.15564	0.2416
590 nm 5 cm	17.20879	-34.6296	28.58512
590 nm 10 cm	5.49434	-12.29547	9.09035
590 nm 30 cm	0.35907	1.65756	0.60337
590 nm 50 cm	0.20783	1.65933	0.35741
590 nm75 cm	0.16851	1.38934	0.29052
590 nm 100 cm	0.14939	1.23197	0.25756
590 nm 200 cm	0.12606	1.03965	0.21735
620 nm 5 cm	0.96643	4.55092	1.63773
620 nm 10 cm	0.61137	4.60489	1.05034
620 nm 30 cm	0.35202	2.90006	0.60694
620 nm 50 cm	0.25702	2.11854	0.44313
620 nm 75 cm	0.16876	1.39151	0.29096
620 nm 100 cm	0.13119	1.08181	0.22618
620 nm 200 cm	0.10155	0.8375	0.17509
660 nm 5 cm	6.72559	33.88354	11.59189
660 nm10 cm	0.95545	7.19627	1.64712
660 nm 30 cm	0.32121	2.64355	0.55382
660 nm 50 cm	0.23002	1.89552	0.39658
660 nm 75 cm	0.17926	1.47785	0.30908
660 nm 100 cm	0.13763	1.1349	0.2373
660 nm 200 cm	0.10576	0.87222	0.18235

Table S45. Relative area of color tunability under different initial concentrations. Mathematical areas of A4 solutions with the initial absorbance between 0.5 and 50 (representing the tunable range of color) under light irradiation.

Maximum Abs.	Mathematical area
A=0.5	757.53
A=1	2315.23
A=2	5489.49
A=4	8901.55
A=6	9846.25
A=8	9692.92
A=10	9122.30
A=25	4839.15
A=50	1335.94

Table S46. Color coordinates of different light sources. *L**, *a**, *b** values of the LEDs with the wavelength of 520, 590, 620 and 660 nm.

Light	*L**	*a**	*b**
520 nm	53.55	-130.17	58.49
590 nm	40.94	23.20	65.50
620 nm	28.21	56.66	42.47
660 nm	10.59	44.62	18.13

Table S47. Color difference between the light source and samples with the initial absorbance at 0.5. Color deviation ($\Delta\theta$) values of A4 solution (initial absorbance=0.5) under light irradiation.

A=0.5	520 nm	590 nm	620 nm	660 nm
5 cm	-42.93	41.55	71.82	61.94
10 cm	-26.43	44.40	70.75	35.00
30 cm	-22.46	54.57	58.74	20.18
50 cm	-20.04	58.92	53.52	18.09
75 cm	-18.91	61.67	50.81	20.26
100 cm	-18.90	63.18	47.09	25.28
200 cm	-18.17	65.22	64.68	49.80

Table S48. Color difference between the light source and samples with the initial absorbance at 1. Color deviation ($\Delta\theta$) values of A4 solution (initial absorbance=1) under light irradiation.

A=1	520 nm	590 nm	620 nm	660 nm
5 cm	-44.25	40.08	69.65	54.80
10 cm	-26.14	43.45	68.35	29.13
30 cm	-22.16	54.86	54.02	17.74
50 cm	-19.72	59.58	48.52	16.48
75 cm	-18.31	62.79	47.26	18.79
100 cm	-18.01	64.71	45.79	24.52
200 cm	-16.69	67.51	70.56	53.72

Table S49. Color difference between the light source and samples with the initial absorbance at 2. Color deviation ($\Delta\theta$) values of A4 solution (initial absorbance=2) under light irradiation.

A=2	520 nm	590 nm	620 nm	660 nm
5 cm	-44.84	39.18	67.23	43.37
10 cm	-24.68	43.42	65.33	22.52
30 cm	-20.80	56.70	45.77	15.51
50 cm	-18.24	62.01	39.80	14.74
75 cm	-16.18	66.25	40.91	16.47
100 cm	-15.19	69.05	43.13	21.92
200 cm	-12.58	73.34	82.11	58.68

Table S50. Color difference between the light source and samples with the initial absorbance at 4. Color deviation ($\Delta\theta$) values of A4 solution (initial absorbance=4) under light irradiation.

A=4	520 nm	590 nm	620 nm	660 nm
5 cm	-42.80	40.72	65.67	30.61
10 cm	-21.14	46.28	62.35	19.27
30 cm	-17.46	61.79	32.94	15.38
50 cm	-14.57	68.03	26.72	13.72
75 cm	-11.16	74.11	28.15	12.81
100 cm	-8.89	78.02	28.54	12.75
200 cm	-4.43	83.13	79.26	32.43

Table S51. Color difference between the light source and samples with the initial absorbance at 6. Color deviation ($\Delta\theta$) values of A4 solution (initial absorbance=6) under light irradiation.

A=6	520 nm	590 nm	620 nm	660 nm
5 cm	-40.06	43.15	65.30	25.98
10 cm	-18.63	49.56	60.43	19.11
30 cm	-15.04	66.09	24.06	14.62
50 cm	-11.85	72.83	16.52	10.39
75 cm	-7.55	79.30	5.98	4.45
100 cm	-4.73	82.75	-8.47	-4.51
200 cm	-0.45	84.74	-19.77	-9.12

Table S52. Color difference between the light source and samples with the initial absorbance at 8. Color deviation ($\Delta\theta$) values of A4 solution (initial absorbance=8) under light irradiation.

A=8	520 nm	590 nm	620 nm	660 nm
5 cm	-37.58	45.49	65.19	23.23
10 cm	-16.97	52.41	58.69	17.45
30 cm	-13.42	69.29	14.54	10.38
50 cm	-10.03	76.12	0.90	1.56
75 cm	-5.29	82.79	-14.23	-6.04
100 cm	-2.00	83.04	-22.30	-9.57
200 cm	-0.53	70.68	-27.26	-13.06

Table S53. Color difference between the light source and samples with the initial absorbance at 10. Color deviation ($\Delta\theta$) values of A4 solution (initial absorbance=10) under light irradiation.

A=10	520 nm	590 nm	620 nm	660 nm
5 cm	-35.48	47.56	65.13	21.18
10 cm	-15.82	54.80	56.96	15.53
30 cm	-12.29	71.81	3.07	4.83
50 cm	-8.69	79.24	-13.66	-5.45
75 cm	-2.99	82.40	-21.39	-8.13
100 cm	-1.08	74.98	-25.23	-10.89
200 cm	-6.18	-7.56	-26.81	-12.26

Table S54. Color difference between the light source and samples with the initial absorbance at 25. Color deviation ($\Delta\theta$) values of A4 solution (initial absorbance=25) under light irradiation.

A=25	520 nm	590 nm	620 nm	660 nm
5 cm	-26.78	57.95	61.17	12.40
10 cm	-10.21	67.08	13.36	-2.80
30 cm	-4.61	77.93	-24.19	-9.35
50 cm	-3.72	29.21	-24.95	-10.18
75 cm	-42.48	-55.76	-25.04	-10.29
100 cm	-131.59	-58.26	-25.04	-10.31
200 cm	-143.35	-58.66	-25.05	-10.31

Table S55. Color difference between the light source and samples with the initial absorbance at 50. Color deviation ($\Delta\theta$) values of A4 solution (initial absorbance=50) under light irradiation.

A=50	520 nm	590 nm	620 nm	660 nm
5 cm	-19.50	69.96	-17.06	-3.23
10 cm	-4.96	73.03	-24.00	-9.22
30 cm	-4.96	-50.50	-25.03	-10.28
50 cm	-118.98	-58.34	-25.04	-10.30
75 cm	-143.58	-58.69	-25.04	-10.30
100 cm	-143.97	-58.69	-25.04	-10.31
200 cm	-144.00	-58.69	-25.04	-10.31

11. Preparation of SAP solutions

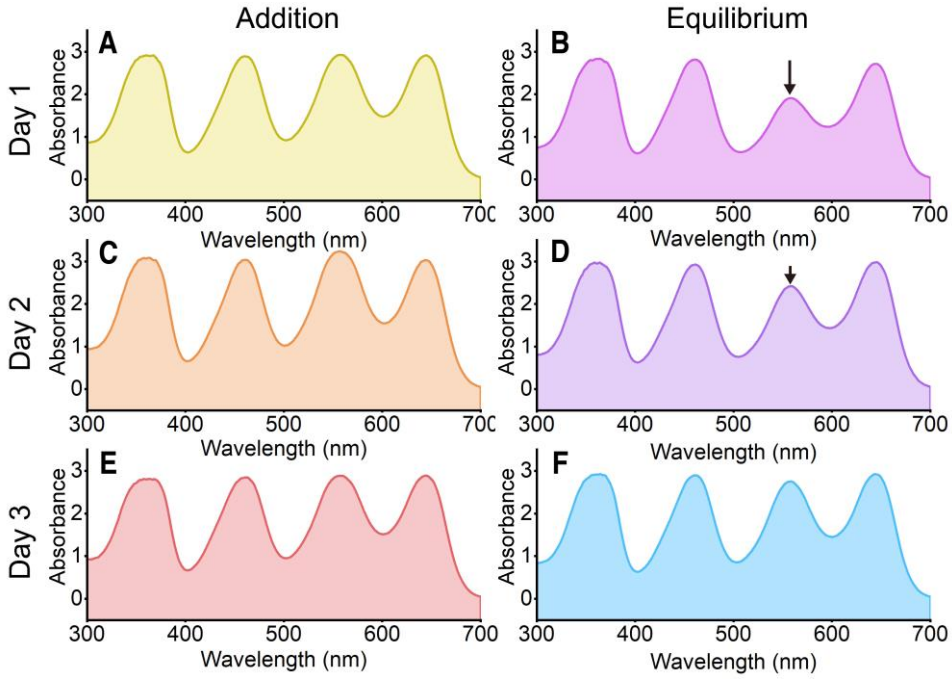

Fig. S28. Absorption spectra of the preparation process of SAP solutions. (**A**, **C** and **E**) UV-vis absorption spectra of the A4 solutions right after adding D1 at day 1, day 2 and day 3, respectively. (**B**, **D** and **F**) UV-vis absorption spectra of the A4 solutions at at day 1, day 2 and day 3, respectively (before adding D1).

12. Processing of the video

Code Environment:
Python=3.7

```
from PIL import Image
import cv2
import numpy as np
import matplotlib.pyplot as plt
from PIL import Image
import cv2
import numpy as np
import matplotlib.pyplot as plt

def calculate_color_distance(color1, color2):
    rmean=(color1[0] - color2[0]) / 2
    r=color1[0] - color2[0]
    g=color1[1] - color2[1]
    b=color1[2] - color2[2]
    distance=np.sqrt(((2 + rmean / 256) * r * r + 4 * g * g + (2 + (255 - rmean) / 256) * b * b))
    return distance

def ave_rgb(im2):
    sum_r2=0
    sum_g2=0
    sum_b2=0
    for y in range(im2.size[1]):
        for x in range(im2.size[0]):
            pix=im2.getpixel((x, y))
            sum_r2=sum_r2 + pix[0]
            sum_g2=sum_g2 + pix[1]
            sum_b2=sum_b2 + pix[2]
    ave_r2=sum_r2 // (im2.size[1] * im2.size[0])
    ave_g2=sum_g2 // (im2.size[1] * im2.size[0])
    ave_b2=sum_b2 // (im2.size[1] * im2.size[0])
    pix0=(ave_r2, ave_g2, ave_b2)
    return pix0

def guiyihua(res):
    result=[]
    for rl in res:
        x=float(rl - np.min(res)) / (np.max(res) - np.min(res))
        result.append(x)
    return result

if __name__ == '__main__':

    video_path=r"D:\color\final.MP4"
```

```
camera=cv2.VideoCapture(video_path)
length=int(camera.get(cv2.CAP_PROP_FRAME_COUNT))
fps=int(camera.get(cv2.CAP_PROP_FPS))
video_time=length // fps
print("length:", length)
print("fps:", fps)
print("time:", video_time)
if not camera.isOpened():
    print("cannot open camera")
    exit(0)

j=0
res_lab=[]
res_lab_c=[]
R=[]
G=[]
B=[]

# loop read video frame
while True:
    ret, frame=camera.read()
    if not ret:
        break

    # left
    pt1=(265, 240)
    pt2=(275, 280)
    cv2.rectangle(frame, pt1, pt2, (0, 255, 0), 1)
    img1=frame[240:280, 265:275]
    cv2.imwrite(r"./left/" + str((j+1)) + '.jpg', img1)

    # mid
    pt1=(265+50, 240)
    pt2=(275+50, 280)
    cv2.rectangle(frame, pt1, pt2, (0, 255, 0), 1)
    img2=frame[240:280, 265+50:275+50]
    cv2.imwrite(r"./mid/" + str((j+1)) + '.jpg', img2)

    # right
    pt1=(265+100, 240)
    pt2=(275+100, 280)
    cv2.rectangle(frame, pt1, pt2, (0, 255, 0), 1)
    img3=frame[240:280, 265+100:275+100]
    cv2.imwrite(r"./right/" + str((j+1)) + '.jpg', img3)

    # color_distance
```

```
    im2=Image.open(r"./mid/" + str((j+1)) + '.jpg')  # 30 110
    pix2=ave_rgb(im2)

    im1=Image.open(r"./left/" + str((j+1)) + '.jpg') # 30 110
    pix10=ave_rgb(im1)

    im3=Image.open(r"./right/" + str((j+1)) + '.jpg') # 30 110
    pix3=ave_rgb(im3)

    R.append(pix2[0]-pix10[0])
    G.append(pix2[1]-pix10[1])
    B.append(pix2[2]-pix10[2])
    distance_lab=calculate_color_distance(pix10, pix2)
    distance_lab_c=calculate_color_distance(pix3, pix2)
    res_lab.append(distance_lab)
    res_lab_c.append(distance_lab_c)
    print(res_lab)
    print(res_lab_c)
    j=j + 1
    cv2.imshow("Camera", frame)
    key=cv2.waitKey(1)
    if key == 27:
        break
cv2.destroyAllWindows()

xaxis=np.linspace(0, video_time ,len(res_lab))
np.savetxt(r'res_lab.txt', res_lab, fmt='%.4f', delimiter=',')
np.savetxt(r'res_lab_c.txt', res_lab_c, fmt='%.4f', delimiter=',')
np.savetxt(r'r.txt', R, fmt='%.4f', delimiter=',')
np.savetxt(r'g.txt', G, fmt='%.4f', delimiter=',')
np.savetxt(r'b.txt', B, fmt='%.4f', delimiter=',')

res_lab_1=guiyihua(res_lab)
res_lab_2=guiyihua(res_lab_c)

plt.figure(1)
plt.plot(xaxis, res_lab_1 ,label="Lab_distance", color='b', linewidth=1)
plt.plot(xaxis, res_lab_2, label="Lab_distance_c", color='r', linewidth=1)
plt.legend()
plt.savefig("lab_distance_final.png")
plt.title("Color_Diff")
plt.xlabel('Time/(s)')
plt.ylabel('Distance')
plt.show()
```

13. SAP coatings

The microscopic images of the A4 paper after spray-coating the SAP coatings for 1, 5 and 10 times are shown in **Fig. S29**. To achieve a black prisine surface, the coating process is needed to be repeated for 10 times.

Due to the rapid evaporation of THF and DCM, uniform porous sturcure was formed on the surface of the film (**Fig. S23A** and **23C**) A rapid annealing process at 150 ^{o}C for 10 s generates relatively tight and smooth surface. (**Fig. S23B** and **23D**).

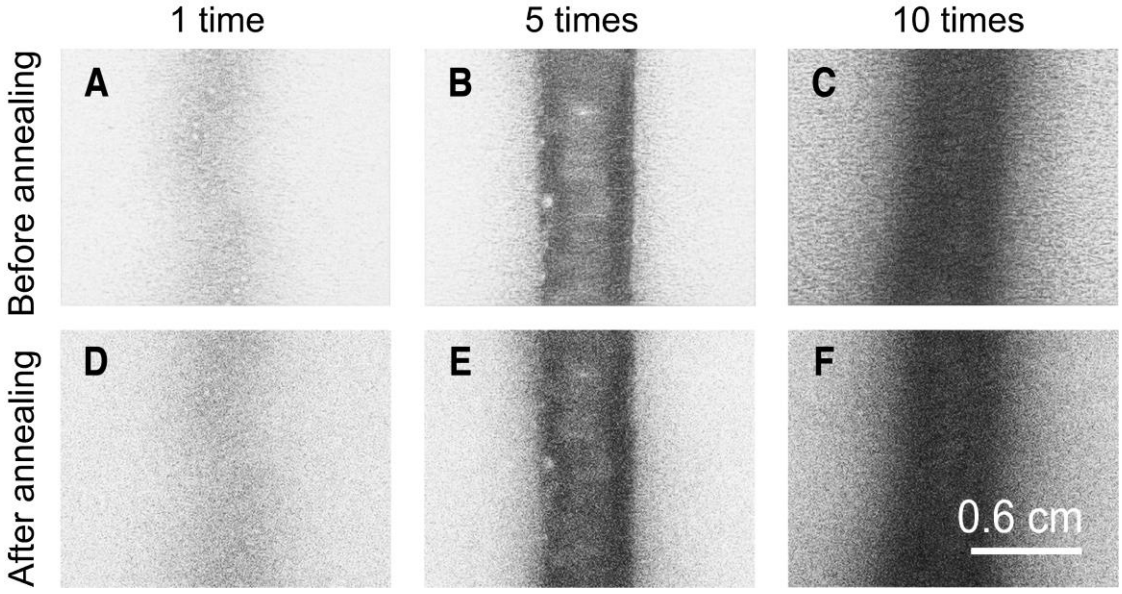

Fig. S29. Images of samples with different spray coating times. Microscopic images of the A4 paper after spray-coating for 1, 5 and 10 times before and after annealing.

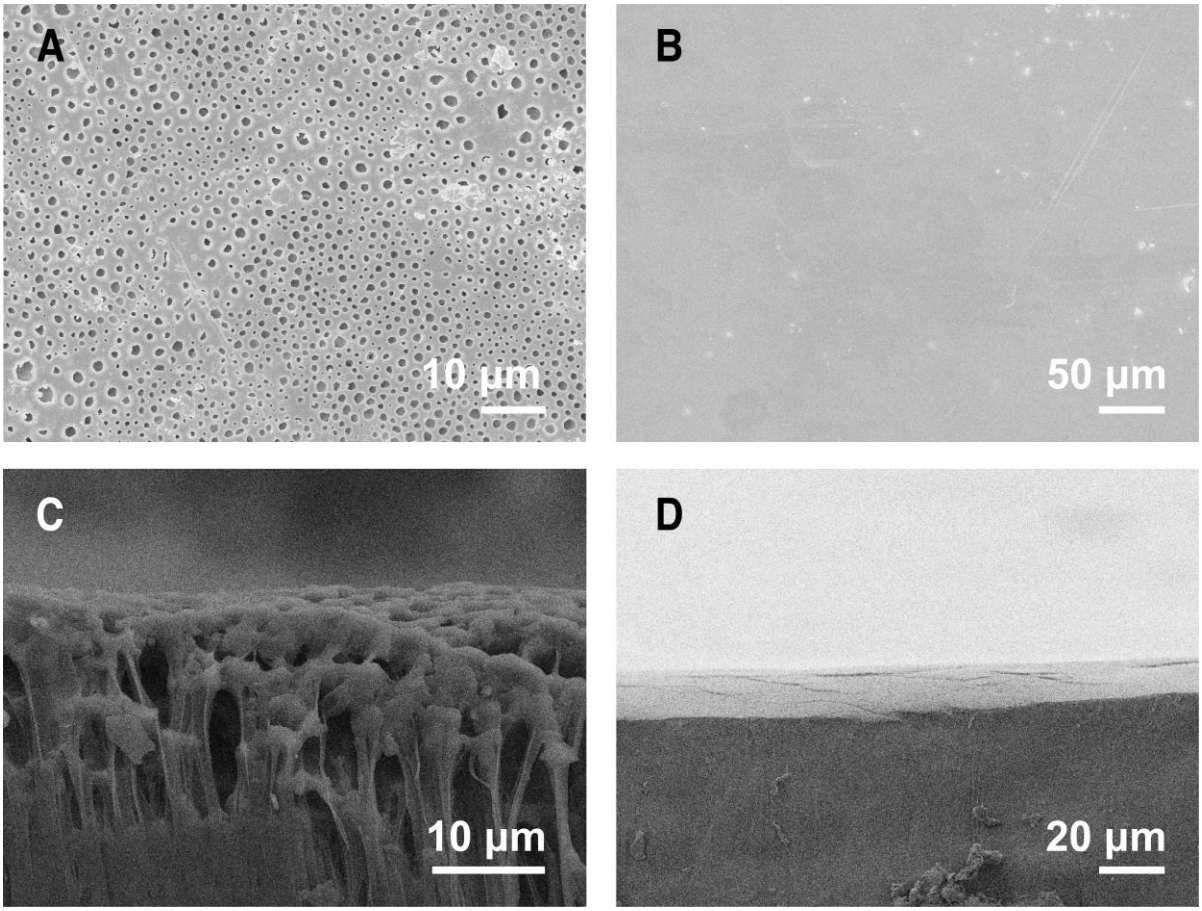

Fig. S30. SEM images of SAP surfaces. (**A**) Top view SEM image of the A4 paper after spray-coating for 10 times before annealing. (**B**) Top view SEM image of the A4 paper after spray-coating for 10 times after annealing. (**C**) Side view SEM image of the A4 paper after spray-coating for 10 times before annealing. (**D**) Side view SEM image of the A4 paper after spray-coating for 10 times after annealing.

14. Supplementary Text

Movies S1 to S9

Movie S1: Active camouflage of SAP solutions in black, red, green, and yellow acrylic boxes.

The left cuvette was loaded with SAP solutions and the right cuvette with black ink as the control. Black dots represent the in situ distance between the average RGB values of regions C and B, and colored dots represent the distance between regions A and B. The movie was speeded up and the timing information of the original movie was embedded in the movie.

Movie S2: Color switching of SAP solutions below black, red, orange, yellow and green acrylic plates.

The SAP solutions were placed below black, red, orange, yellow and green arylic plates. The movie was speeded up and the timing information of the original movie was embedded in the movie.

Movie S3: Color switching of SAP solutions in red, green and yellow bushes.

The SAP solutions were placed in red (*Cyclamen persicum*), green (*Epipremnum aureum*) and yellow (*Ginkgo*) bushes, and a white light LED was set to the left of the plants. The movie was speeded up and the timing information of the original movie was embedded in the movie.

Movie S4: Color switching of SAP solutions below red petal, green leaf and yellow leaf.

SAP solutions were placed below red petal, green leaf and yellow leaf. The movie was speeded up and the timing information of the original movie was embedded in the movie.

Movie S5: Color switching of SAP solutions under red, orange, yellow and green umbrellas.

SAP solutions were set under red, orange, yellow and green umbrellas, respectively, which were put under sunlight (60000 lux, 37 °C, and bottles were stored in the dark and immersed in liquid nitrogen for 5 s before the experiments). The movie was speeded up and the timing information of the original movie was embedded in the movie.

Movie S6: Active camouflage of SAP solutions under red, orange, yellow and green umbrellas.

SAP solutions were set under a red umbrella, which were put under sunlight (60000 lux, 37 °C, and bottles were stored in the dark and immersed in liquid nitrogen for 5 s before the experiments). The umbrella was changed by yellow and green umbrellas sequentially. The movie was speeded up and the timing information of the original movie was embedded in the movie.

Movie S7: Active camouflage of SAP solutions in NMR tube below sequentially arranged sticky notes.

SAP solution was filled into a NMR tube, which was covered with sequentially arranged red, green and yellow sticky notes. A white light LED was set on the top. The movie was speeded up and the timing information of the original movie was embedded in the movie.

Movie S8: Color switching of SAP films upon light irradiation with corresponding wavelength.

SAP films were irradiated by 660, 520 and 590 nm light irradiation, respectively. The movie was speeded up and the timing information of the original movie was embedded in the movie.

Movie S9: Color switching of ABS models upon light irradiation with corresponding wavelength.

ABS models coated with SAP coatings were irradiated by 660, 520 and 590 nm light irradiation, respectively. The movie was speeded up and the timing information of the original movie was embedded in the movie.

Data S1 to S2

Data S1: Raw data from Fig. 2 and the conversion process from the absorption spectra (300-800 nm) to the corresponding color coordinates.

Data S2: Raw data from Fig. S19-S27, Fig. 3A, and Fig. S4C, along with the conversion process from the absorption spectra (300-800 nm) to the corresponding color coordinates.